Wave Packet Dynamics in Time-Dependent Quantum Systems

Candidate Number: 1092139

A thesis submitted in partial fulfilment of the requirements for the degree of

Master of Science in Theoretical and Computational Chemistry

August 2025

Acknowledgements

I wish to convey my sincere thanks and gratitude to my lecturers on this Master's programme who have delivered an academically rigorous, challenging, and thus hugely enjoyable course. It has provided me with a deep appreciation and comprehensive understanding of fundamental topics in the field of theoretical and computational chemistry. In particular, I would like to thank Prof Adam Kirrander for his thoughtful and considered supervision throughout my summer research project.

My time at the University of Oxford simply would not have been possible without the steadfast support of my family, whom I am indebted to for their endless love, counsel and encouragement, which has allowed me to pursue my goals, both academic and personal, with conviction and to the best of my ability. I am forever grateful for the sacrifices they have made that have afforded me such a happy, stable, and enriching upbringing, in addition to an education that has given me invaluable knowledge and skills for life.

Finally, my Oxford experience would not have been anywhere near as memorable without my wonderful friends, who have brought such joy to my time at the University. Their individuality and perspective on life and the world, good-natured and bubbly personalities, and dedication to their respective disciplines has been, and continues to be, inspiring, and has certainly contributed in no small part to making my time at Oxford one of the best years of my life.

To you all – thank you!

Contents

1 Introduction

Whilst a wealth of insight into the behaviour of quantum systems can be obtained by probing solutions to the time-independent Schrödinger equation, the most general solutions can be obtained by considering the time-dependent Schrödinger equation (TDSE). As prominent topics in chemical physics such as chemical reaction dynamics, spectroscopy, photochemical processes, electronic structure theory, and molecular quantum dynamics are inherently time-dependent, one turns to study the time-dependence of wavefunctions to understand a system's temporal behaviour. This naturally leads to the study of solutions to the TDSE and linear combinations of such solutions to form wave packets, thus laying the foundations for the calculation of the physical properties of quantum systems, in addition to providing insight into how observables depend on time.

The development of theory is key to rationalising experimental observations and making predictions to guide areas of future research. The concept of a wave packet is particularly useful when studying quantum dynamics, which will be explored extensively in this thesis. Wave packets can be exploited to gain a comprehensive overview of reaction dynamics. Simmermacher *et al* have shown that x-ray scattering from molecular wave packets can elucidate key insights into dynamics beyond those that are structural by studying the elastic, inelastic and mixed coherent mixed scattering signals.[1] In addition, the theory of wave packets can also be applied to the study of molecular photodissociation, by mapping nonadiabatic transitions at avoided crossings and probing electron coherence via electron scattering, as shown by Liane *et al.*[2] Wave packets can be manipulated through chirping, which allows for a wave packet to be focused, say, on a particular region of a potential

energy surface, or to engineer specific quantum dynamics for a desired application, for example investigating the quantum behaviour of molecules at a transition state,[3] **(NEED TO CHECK THE RELEVANCE OF REFERENCE** or population inversion in laser physics.[4]

There are several methods by which the TDSE can be solved. Grid-based methods involve discretising a system of interest in space, and time and then numerically solving the TDSE at each point in the discretisation. The split operator,[5] Crank-Nicolson,[6,7] and finite difference methods to approximate continuous derivatives are grid-based methods that are commonly adopted. The multiconfiguration time-dependent Hartree (MCTDH) approach uses a wavefunction ansatz of a linear combination of Hartree products.[8,9] This combines the computational scaling benefits enjoyed by self-consistent field methods, with the numerical exactness of traditional approaches of wavefunction time propagation, by multiplying solutions to the time-independent Schrödinger equation (TISE) by $\exp(-iEt/\hbar)$, where E is the energy of the time-independent solution. Finally, quantum-classical methods are popular when treating chemical systems: electrons are given a full quantum mechanical treatment, whereas nuclei are treated using classical dynamics owing to their significantly larger mass and longer timescales of motion. **(NEED A REFERENCE HERE - ASK GROUP)**

This thesis presents a thorough investigation into methods to solve the TDSE, in addition to exploring the time-evolution of quantum systems via wave packet dynamics. To supplement theoretical calculations, MATLAB scripts have been developed to aid the interpretation and understanding of the underlying physics of time-dependent quantum mechanics. In Chapter 2, the general theory of the TDSE, the separation of variables method as a means to solve it, and properties of general solutions are explored. This includes how observables, expectation values and flux can be readily obtained from these solutions. Next, Chapter 3 discusses the theory of the Crank-Nicolson and split operator methods, and how they are applicable to solving the TDSE, as well as offering a critical evaluation of each method's suitability to wave packet propagation. Chapter 4 investigates the quantum dynamics of the particle in a box and Quantum Harmonic Oscillator (QHO), by probing the behaviour of linear superpositions of each respective system's eigenstates and the corresponding probability density function. The focus of the thesis then shifts to the analysis of Gaussian wave packets expressed as an integral of free particle eigenstates over all momentum space, which is the subject of Chapter 5. Specifically, the physical properties of Gaussian wave packets as they evolve over time, as well as the interference between travelling wave packets, are considered.

The thesis closes with an examination of chirping a Gaussian wave packet with a polynomial phase as a means to manipulate its behaviour in Chapter 6.

All simulations performed using MATLAB scripts can be accessed via GitHub in the following repository: https://github.com/MaxButterworth/MSc-Project.git
DO I NEED TO REMOVE THIS LINK BECAUSE OF ANONYMITY?

2 Theory

2.1 The Time-Dependent Schrödinger Equation

The non-relativistic single-particle TDSE, given by

$$i\hbar\frac{\partial\psi(\mathbf{x},t)}{\partial t} = \left[-\frac{\hbar^2}{2m}\nabla^2 + V(\hat{\mathbf{x}},t)\right]\psi(\mathbf{x},t), \tag{2.1}$$

where m denotes mass, governs how a quantum system subjected to a potential $V(\hat{\mathbf{x}},t)$ and described by a wavefunction $\psi(\mathbf{x},t)$, with $\mathbf{x} = \begin{pmatrix} x & y & z \end{pmatrix}^{\mathrm{T}}$, evolves over space and time. The non-relativistic Hamiltonian operator in its most general form is time-dependent, and defined as

$$\hat{H}(\mathbf{x},t) = -\frac{\hbar^2}{2m}\nabla^2 + V(\hat{\mathbf{x}},t). \tag{2.2}$$

However, many quantum systems that are ubiquitous in the field of chemical physics are described by time-independent Hamiltonians, so for the purposes of this thesis the Hamiltonian is assumed to be time-independent with $\hat{H} = \hat{H}(\mathbf{x})$ unless otherwise stated. For clarity, the one-dimensional case will be considered henceforth, but one can straightforwardly generalise the theory to the three-dimensional case.

According to the conventional interpretation of the wavefunction by Born, its square norm represents a probability density. For instance, if the wavefunction $\psi(x,t)$ describes a quantum particle, then the probability of finding the particle within a spatial region $\tilde{x} \to \tilde{x} + dx$ at time t_0 is simply $|\psi(\tilde{x},t_0)|^2 dx$. This interpretation of the wavefunction implicitly assumes that $\psi(x,t)$ is suitably normalised such that

$$\int_{-\infty}^{\infty} |\psi(x,t)|^2 \, dx = 1. \tag{2.3}$$

2.1.1 Separation of Variables

The set of particular solutions to a TDSE with a time-independent Hamiltonian may be obtained via the separation of variables method. To begin, the following product ansatz for the wavefunction is adopted:

$$\psi(x,t) = \alpha(x)\beta(t). \tag{2.4}$$

Substituting Equation 2.4 into Equation 2.1 with the Hamiltonian given by Equation 2.2 yields:

$$i\hbar\frac{\partial\psi(x,t)}{\partial t} = \hat{H}\psi(x,t) \tag{2.5}$$

$$\implies i\hbar\frac{\partial}{\partial t}\left(\alpha(x)\beta(t)\right) = \hat{H}\left(\alpha(x)\beta(t)\right) \tag{2.6}$$

$$\implies i\hbar\frac{1}{\beta(t)}\frac{\partial\beta(t)}{\partial t} = \frac{1}{\alpha(x)}\hat{H}\alpha(x). \tag{2.7}$$

Assuming that $\alpha(x)$ is an eigenstate of the Hamiltonian, the right hand side of Equation 2.7 is equal to a constant describing the energy of the eigenstate, E. This now gives rise to two differential equations that can be solved independently:

$$\hat{H}\alpha(x) = E\alpha(x) \tag{2.8}$$

$$i\hbar\frac{\partial\beta(t)}{\partial t} = E\beta(t). \tag{2.9}$$

Equation 2.8 is the time-independent Schrödinger equation with the solution $\alpha(x)$, and Equation 2.9 is a separable first-order linear ordinary differential equation that can be readily solved to obtain

$$\beta(t) = \beta_0 e^{-iEt/\hbar}. \tag{2.10}$$

The overall solution

$$\psi(x,t) = \beta_0\alpha(x)e^{-iEt/\hbar} \tag{2.11}$$

is a *particular solution* to Equation 2.5.

2.1.2 General Solutions of the Time-Dependent Schrödinger Equation

The most general solution of the TDSE (Equation 2.5), $\Psi(x,t)$, is a linear superposition of all particular solutions. If a Hamiltonian has complete basis of normalised eigenstates with an arbitrary quantum number n given by $\{|\phi_n\rangle : \forall\ n\}$,

with corresponding energies $\{E_n : \forall\ n\}$, then for a bounded system the general solution takes the form of a discrete sum:

$$\Psi(x,t) = \sum_{n=1}^{\infty} c_n |\phi_n\rangle e^{-iE_n t/\hbar}, \tag{2.12}$$

where c_n is the coefficient of $|\phi_n\rangle$ in the expansion. On the other hand, for unbounded systems, the spectrum of eigenstates forms a continuum and the general solution may expressed as an integral over energy (or other suitable variable):

$$\Psi(x,t) = \int_0^{\infty} c(E) |\phi_E\rangle e^{-iEt/\hbar}\, dE, \tag{2.13}$$

where $c(E)$ is the spectral distribution of energies.

Consider again Equation 2.11. The corresponding probability density can be easily calculated to give

$$|\psi(x,t)|^2 = |\beta_0 \alpha(x)|^2 . \tag{2.14}$$

Equation 2.14 is clearly time independent and hence $\psi(x,t)$ is known as a stationary state. This is a profound result indicating that the probability of finding a particle at a particular point in space does not change with time, because the time-dependence of ψ is contained in the complex phase term. However, the probability density of a superposition state, the simplest of which is given by

$$\left|\tilde{\psi}\right\rangle = c_1 |\phi_1\rangle e^{-iE_1 t/\hbar} + c_2 |\phi_2\rangle e^{-iE_2 t/\hbar}, \tag{2.15}$$

does vary with time. This can be seen by considering the square norm of Equation 2.15 in the position representation,:

$$\left|\tilde{\psi}(x,t)\right|^2 = |c_1|^2 |\phi_1(x)|^2 + |c_1|^2 |\phi_2(x)|^2 + 2\mathrm{Re}\left[c_1^* c_2 \phi_1^*(x) \phi_2(x) e^{-i(E_2 - E_1)t/\hbar}\right], \tag{2.16}$$

The probability density of the superposition state given by Equation 2.16 has its time-dependence contained in the phase term $\exp\left(-i(E_2 - E_1)t/\hbar\right)$; this is attributable to the coupling of $\phi_1(x)$ and $\phi_1(x)$. Indeed, any superposition of eigenstates gives rise to time-dependent probability densities and observables. In other words, a superposition of stationary states forms a non-stationary state. Consequently, the probability density, a real quantity, oscillates with a period equal to $(E_1 - E_2)/\hbar$.

2.2 Measurement in Quantum Mechanics

2.2.1 Observables

Observable quantities are represented by Hermitian operators because these necessarily admit real eigenvalues. Given an arbitrary hermitian operator $\hat{A}$ with eigenvalues a_n corresponding to the observable A, by the spectral theorem the eigenvectors of the matrix representation of $\hat{A}$ form an orthonormal basis $\{|\chi_i\rangle : \forall\ i\}$. There are two scenarios to consider when $\hat{A}$ acts on the state $|\psi_n\rangle$:

1. $|\psi_n\rangle = |\chi_n\rangle$, an eigenstate of $\hat{A}$. In this instance
$$\hat{A}|\psi_n\rangle = \hat{A}|\chi_n\rangle = a_n|\chi_n\rangle = a_n|\psi_n\rangle \tag{2.17}$$
and the value of A for the state $|\psi_n\rangle$ is readily recovered.

2. $|\psi_n\rangle$ is not an eigenstate of $\hat{A}$. By virtue of the spectral theorem, $|\psi_n\rangle$ may be expressed as a linear combination of the eigenstates of $\hat{A}$; $|\psi_n\rangle$ does not have a definite value of A. Thus, the action of $\hat{A}$ on $|\psi_n\rangle$ gives
$$\hat{A}|\psi_n\rangle = \hat{A}\sum_{i=1}^{\infty} c_i|\chi_i\rangle = \sum_{i=1}^{\infty} c_i a_i|\chi_i\rangle, \tag{2.18}$$
which is a weighted sum of the eigenfunctions of $\hat{A}$ with each term multiplied by its respective eigenvalue. Making a measurement of A will collapse $|\psi_n\rangle$ into a single eigenstate of $\hat{A}$ with probability $|c_i|^2$.

In both scenarios above, if $\{|\chi_i\rangle : \forall\ i\}$ is a set of time-dependent eigenstates, then whilst the relevant eigenvalues are still recovered, the states will continue to evolve according to the TDSE after a measurement has taken place. However, these states are stationary and so each has a time-independent probability density function.

2.2.2 Expectation Values

One may ask what is the average value of an observable for a given quantum system. In this instance, the expectation value is calculated, which takes the general form
$$\langle A\rangle = \left\langle \psi \left| \hat{A} \right| \psi \right\rangle. \tag{2.19}$$
The time derivative of an expectation value is easily calculated using the Ehrenfest theorem:
$$\frac{d\langle A\rangle}{dt} = \frac{i}{\hbar}\left\langle \left[\hat{H}, \hat{A}\right] \right\rangle + \left\langle \frac{\partial \hat{A}}{\partial t} \right\rangle, \tag{2.20}$$
where $[\hat{H}, \hat{A}] = \hat{H}\hat{A} - \hat{A}\hat{H}$ is the commutator of the Hamiltonian and $\hat{A}$. If $\hat{A}$ is time-independent, Equation 2.20 simplifies to
$$\frac{d\langle A\rangle}{dt} = \frac{i}{\hbar}\left\langle \left[\hat{H}, \hat{A}\right] \right\rangle. \tag{2.21}$$

2.2.3 Flux

Flux, J, also known as the probability current, measures the flow of probability over space and time. The flux at a point $x = s$ is calculated by taking the expectation value of the Heisenberg time derivative of the projection onto the subspace where $x > s$, that is

$$\hat{F}(s,t) = \frac{i}{\hbar}\left[\hat{H}, h(\hat{x}-s)\right], \tag{2.22}$$

where

$$h(\hat{x}-s) = \begin{cases} 1, & x \geq s \\ 0, & x < s \end{cases} \tag{2.23}$$

is the Heaviside step function. In one dimension, Equation 2.22 may be expressed as

$$\hat{F}(s,t) = \frac{i}{\hbar}\left[\frac{\hat{p}^2}{2m}, h(\hat{x}-s)\right] \tag{2.24}$$

$$\implies \hat{F}(s,t) = \frac{i}{2m\hbar}\left\{\hat{p}\left[\hat{p}, h(\hat{x}-s)\right] + \left[\hat{p}, h(\hat{x}-s)\right]\hat{p}\right\}. \tag{2.25}$$

Now, given that

$$[\hat{p}, h(\hat{x}-s)] = -i\hbar\delta(\hat{x}-s), \tag{2.26}$$

Equation 2.25 can be written as

$$\hat{F}(s,t) = \frac{1}{2m}\left\{\hat{p}\delta(\hat{x}-s) + \delta(\hat{x}-s)\hat{p}\right\} \tag{2.27}$$

$$\implies \hat{F}(s,t) = -\frac{i\hbar}{2m}\left\{\frac{d}{dx}\delta(x-s) + \delta(x-s)\frac{d}{dx}\right\}. \tag{2.28}$$

Thus, the flux of the eigenstate $|\psi(x,t)\rangle$ is given by

$$J(s,t) \equiv \left\langle \psi(x,t) \middle| \hat{F} \middle| \psi(x,t) \right\rangle = -\frac{i\hbar}{2m}\int_{-\infty}^{\infty} \psi^*(x,t)\hat{F}\psi(x,t)\ dx. \tag{2.29}$$

Next, substituting Equation 2.28 into Equation 2.29 (where $\psi(x,t) \equiv \psi$ for clarity) yields

$$J(s,t) = -\frac{i\hbar}{2m}\int_{-\infty}^{\infty} \psi^*\frac{d}{dx}\left[\delta(x-s)\psi\right] + \psi^*\delta(x-s)\frac{d\psi}{dx}\ dx. \tag{2.30}$$

The first term in the integrand of Equation 2.30 may be integrated by parts, so Equation 2.30 becomes

$$J(s,t) = -\frac{i\hbar}{2m}\left\{\psi^*\frac{d\psi}{dx} + \left[\delta(x-s)\psi^*\right]_{-\infty}^{\infty} - \int_{-\infty}^{\infty}\frac{d\psi^*}{dx}\delta(x-s)\psi\ dx\right\}. \tag{2.31}$$

By virtue of the properties of the Dirac delta function, coupled with the fact that the wavefunction vanishes in the limit of $|x| \to \infty$, one finally obtains

$$J(s,t) = \frac{i\hbar}{2m}\left\{\frac{d\psi^*}{dx}\psi(x,t) - \psi^*(x,t)\frac{d\psi}{dx}\right\}. \tag{2.32}$$

A comforting result is that Equation 2.32 satisfies the continuity equation, that is

$$\frac{\partial J(s,t)}{\partial s} - \frac{\partial}{\partial t}\left|\psi(s,t)\right|^2 = 0 \tag{2.33}$$

demonstrating the conservation of probability as closed quantum systems that evolve unitarily according to an Hermitian Hamiltonian.

2.3 Wave Packets

A wave packet is an incredibly useful and versatile tool to probe time-dependent quantum mechanics as they can be localised in space and propagated through time, and used to study interference with other wave packets, say for two coupled quantum states. Generally speaking, a wave packet is formed by an arbitrary linear superposition of solutions to the TDSE. The superposition can take two forms:

1. A discrete sum if the solutions to the TDSE form a discrete basis set, an example of which is Equation 2.12;

2. A continuous integral if the solutions to the TDSE form a continuum, such as Equation 2.13.

Equation 2.19 can be utilised to calculate the position of the centre of the wave packet to give

$$\langle x\rangle_t = \int_{-\infty}^{\infty} x\left|\psi(x,t)\right|^2\ dx; \tag{2.34}$$

it is assumed that $\psi(x,t)$ is normalised. Secondly, the group velocity of a wave packet describing how quickly its centre moves through space is given by

$$v_g = \frac{\partial\omega}{\partial k}, \tag{2.35}$$

where ω and k are the angular frequency and wavenumber of the wave packet, respectively. Thirdly, the phase velocity, describing the velocity of individual waves that comprise the wave packet, is defined as

$$v_p = \frac{\omega}{k}. \tag{2.36}$$

Some fundamental properties of wave packets are well-described by classical equations of motion. It will be shown in Chapter 5 that this indeed the case for the average position, group velocity and phase velocity of a free particle wave packet. This correspondence principle affords a greater level of physical intuition when interpreting the results of quantum mechanics when viewed through the lens of propagating wave packet.

Another useful property of wave packets is that they manifestly encode the Heisenberg uncertainty principle:

$$\Delta x \Delta k \geq \frac{\hbar}{2} \tag{2.37}$$

This can most readily be seen by considering the following arbitrary Gaussian wave packet in real space given by

$$\psi(x) = N \int_{-\infty}^{\infty} e^{-(k-k_0)^2/2\sigma^2} e^{ikx}\ dk, \tag{2.38}$$

where N is a normalisation constant, and σ and k_0 is the width and the centre of the Gaussian function, respectively. Equation 2.38 may be viewed as the inverse Fourier transform of the Gaussian function $g(k) = e^{-(k-k_0)^2/2\sigma^2}$. Evaluating Equation 2.38 gives the following result:

$$\psi(x) = sNe^{-\sigma^2 x^2/2} e^{ik_0 x}. \tag{2.39}$$

Like g, Equation 2.39 is also a Gaussian function with a width $1/\sigma$. This demonstrates that a narrow Gaussian wave packet in real space results in a wider Gaussian packet in momentum space and vice versa. Notice also how the shift in the initial centre of the wave packet in k-space, described by Equation 2.38, vanishes when the integral is calculated to yield Equation 2.39, the time evolution of which is described by:

$$\psi(x,t) = sNe^{\left[-\sigma^2 x^2/2\right] + [iEt/\hbar]} e^{ik_0 x}, \tag{2.40}$$

where E is the energy of the state ψ.

3

Numerical Methods to Solve the Time-Dependent Schrödinger Equation

In practice, it is more favourable to solve the TDSE using numerical methods rather than their analytical counterparts. This is primarily because the TDSE is analytically soluble for all but the most simple of systems, and thus analytical methods are seldom useful when one wishes to treat complex molecular systems. Two methods will be discussed: the Crank-Nicolson (CN) method and the split operator (SO) method.

3.1 The Crank-Nicolson Method

The CN method, accurate to second order in time, is an implicit method that exploits finite difference approaches to approximate derivatives, and hence solve the TDSE.[6] It is particularly suited to computational applications owing to the fact that the method relies on solving systems of linear equations which may be encoded as a simple matrix equation.

The finite difference method for approximating the first derivative of the wavefunction with respect to time, and second derivative of the wavefunction with respect to x is given by

$$\frac{\partial\psi(x,t)}{\partial t} \approx \frac{\psi(x,t+\Delta t)-\psi(x,t)}{\Delta t} \tag{3.1}$$

and

$$\frac{\partial^2\psi(x,t)}{\partial x^2} \approx \frac{\psi(x-\Delta x,t)-2\psi(x,t)+\psi(x+\Delta x,t)}{\Delta t^2}, \tag{3.2}$$

respectively, which both become exact in the limit that $\Delta t \to 0$. Next, the CN method involves solving the following equation for $\psi(x, t + \Delta t)$:

$$\left[1 + \frac{i\Delta t}{2\hbar}\hat{H}\right]\psi(x, t + \Delta t) = \left[1 - \frac{i\Delta t}{2\hbar}\hat{H}\right]\psi(x, t). \tag{3.3}$$

Computationally, this is most easily achieved by encoding Equation 3.3 in matrix form as

$$\boldsymbol{A}|\psi_{t+\Delta t}\rangle = \boldsymbol{B}|\psi_t\rangle, \tag{3.4}$$

with

$$\boldsymbol{A} = \boldsymbol{I_n} + \frac{i\Delta t}{2\hbar}\boldsymbol{H} \tag{3.5}$$

and

$$\boldsymbol{B} = \boldsymbol{I_n} - \frac{i\Delta t}{2\hbar}\boldsymbol{H}, \tag{3.6}$$

where $\boldsymbol{I_n}$ is the $n \times n$ identity matrix, $\boldsymbol{H}$ is the Hamiltonian matrix, and $|\psi_t\rangle$ is a column vector describing the wave packet at time t. Hence, the state of the wave packet at a time $t + \Delta t$ is given by

$$\psi_{t+\Delta t} = \boldsymbol{A^{-1}B}|\psi_t\rangle. \tag{3.7}$$

3.2 The Split Operator Method

The approach of the SO method, which can be regarded as a pseudo-spectral method to solve differential equations, is to approximate the time propagator as

$$U(x, t) = e^{\left(-i\hat{H}t/\hbar\right)} = \underbrace{e^{\left(-i\hat{H}\Delta t/\hbar\right)}e^{\left(-i\hat{H}\Delta t/\hbar\right)}\ldots e^{\left(-i\hat{H}\Delta t/\hbar\right)}}_{\text{n iterations}}, \tag{3.8}$$

where $t = \sum_{i=1}^{n}\Delta t$.[5] Owing to the fact that the kinetic energy and potential energy operators do not commute, one can proceed by expanding the Hamiltonian using the Baker-Campbell-Hausdorff formula:

$$e^{\left(-i\hat{H}\Delta t/\hbar\right)} \approx e^{\left(-i\hat{T}\Delta t/\hbar\right)}e^{\left(-iV(\hat{x})\Delta t/\hbar\right)} + \mathcal{O}\left(\Delta t^2\right). \tag{3.9}$$

The approximation in Equation 3.9 affords reasonable accuracy provided that the timestep, Δt is sufficiently small because the error is proportional to $\left[\hat{T}, V(\hat{x})\right]$ and on the order of Δt^2. Once can show this by expanding the left hand and right hand sides of Equation 3.9 and comparing the results. However, the error can be improved upon should a greater level of accuracy be required for numerical calculations.

To make progress, one can exploit Strang splitting by taking the symmetrised product of both exponential kinetic and potential energy operators to reduce the order of the error on the expansion to Δt^3:

$$e^{\left(-i\hat{H}\Delta t/\hbar\right)} = \left[e^{(-iV(\hat{x})\Delta t/2\hbar)}e^{\left(-i\hat{T}\Delta t/2\hbar\right)}\right]\left[e^{\left(-i\hat{T}\Delta t/2\hbar\right)}e^{(-iV(\hat{x})\Delta t/2\hbar)}\right] \tag{3.10}$$

$$= e^{(-iV(\hat{x})\Delta t/2\hbar)}e^{\left(-i\hat{T}\Delta t/\hbar\right)}e^{(-iV(\hat{x})\Delta t/2\hbar)} + \mathcal{O}\left(\Delta t^3\right). \tag{3.11}$$

When implementing Equation 3.11 in practice, it is more convenient to perform the half-step operation in real space and the full-step operation in momentum space, recalling that $\hat{T} = \frac{\hat{p}^2}{2m}$ where the eigenvalues of $\hat{p}$ are $p = \hbar k$. The fast Fourier transform (FFT) algorithm is an efficient way to move between real and momentum space without noticeably hindering the speed of computational calculations.

3.3 Evaluation of Numerical Methods

Whilst both the CN and SO methods are valid approaches to solve the TDSE, the latter is superior in terms of accuracy. The CN method is not symplectic, that is it does not conserve phase space volumes, but it is unitary because, in light of Equation 3.7,

$$\boldsymbol{A^{-1}B(A^{-1}B)^{-1} = A^{-1}BB^{-1}A = I_n}, \tag{3.12}$$

thus demonstrating that the norm squared of a wavefunction being propagated using the CN method is preserved throughout. In addition, the method is unconditionally stable meaning the algorithm is numerically stable no matter the duration of a single timestep, and correct to second order in space and time. Despite this, the CN method is prone to phase error accumulation rendering it insufficient when propagating wave packets: such deficiencies hinder the study of dispersion, group velocities and phase velocities where accurate phase information is crucial, and thus needs to be preserved. Such phenomena will be analysed in Section 3.4 using MATLAB simulations. On balance the CN method is suitable when rapid approximations of how a wavefunction would evolve over time according to the TDSE are required, rather than extremely precise calculations. In spite of this, research has been conducted which improves upon the method presented in Section 3.1, particularly in relation to quantum tunnelling applications.[7]

The SO method is also unitary and has the advantage that it is an explicit method in time, so a set of linear equations need not be solved to obtain a solution which is in contrast to the implicit nature of the CN. As such, the SO method

improves tractability when applied to more complex quanutm systems. Where the SO method especially shines, is when an operator can be written as a sum of operators that either depend on the canonical variables of position and momentum – the Hamiltonian fulfils this criterion. Furthermore, deploying the FFT algorithm means the exponentiation of the Hamiltonian is more efficient compared to matrix diagonalisation, which is of particular importance for systems where the Hamiltonian matrix is dense.[10] Critically, the SO method does not suffer from the same phase accumulation issues identified for the CN Method; this is explicitly demonstrated in Section 3.4. One is not necessarily restricted to using free particle wavefunctions as the basis set for the SO method. Rather, any spectral basis set can be adopted assuming that the FFT is substituted for the appropriate spectral transformation.

One disadvantage of the SO method is that it implicitly assumes that periodic boundary conditions are applicable to the system when using the FFT to switch between real and reciprocal space. Consequently, it does not perform well for systems such as the particle in a box where the boundary conditions are not periodic. The results presented in Section 4.2 rely on the CN method as the SO method performs poorly due to high levels of numerical noise originating from the boundaries of the infinite potential well. However, the simulations conducted for all other systems analysed used the SO method to propagate the wave packet.

3.4 Verification of the Split Operator Method Implementation in MATLAB Simulations

The MATLAB simulations, which propagated wavefunctions using the split operator method to generate the results of Section 4.3, Chapter 5, and Chapter 6, were checked and verified using the analytical equations for wave packet propagation derived in Chapter 1 and Section 5.1. Two wave packets, both with the same initial conditions, were simulated independently: the first, $\psi_{\text{numerical}}(x,t)$, was propagated through time numerically using the SO method and the second, $\psi_{\text{analytical}}(x,t)$, was propagated through time analytically.

The accuracy of the SO method was quantified by determining the error on the following quantities:

1. The norm squared value of the difference between the real and imaginary parts of $\psi_{\text{numerical}}(x,t)$ and $\psi_{\text{analytical}}(x,t)$. This was calculated using the following equation:

$$|\Delta\psi(x,t)|^2 = |\psi_{\text{numerical}}(x,t) - \psi_{\text{analytical}}(x,t)|^2 \tag{3.13}$$

The aim of this calculation was to assess whether the values of both the real and imaginary parts of the numerically propagated wave packet were accurate over time.

2. The error on the average position,

$$\Delta\langle x\rangle_t = \langle x\rangle_{\text{t, numerical}} - \langle x\rangle_{\text{t, analytical}}, \tag{3.14}$$

to ensure that the numerical propagation through time leads to the correct group velocity and phase velocities (and hence dispersion).

3. The overlap between the wave packets given by

$$\langle\psi_{\text{numerical}}|\psi_{\text{analytical}}\rangle_t = \int_{-\infty}^{\infty} \psi^*_{\text{numerical}}(x,t)\psi_{\text{analytical}}(x,t)\ dx. \tag{3.15}$$

This quantity measures the degree to which both the numerically propagated wave packet agrees with the analytical result in its entirety.

4. The error in group velocity over time,

$$\Delta v_g(t) = v_{g,\text{ numerical}}(t) - v_{g,\text{ analytical}}(t). \tag{3.16}$$

5. The error in dispersion over time,

$$\Delta(\Delta x)(t) = \Delta x_{\text{numerical}}(t) - \Delta x_{\text{analytical}}(t). \tag{3.17}$$

This metric will quantify how accurately phase velocities of the different free particle basis functions are propagated over the course of the simulation.

Parameter	Assigned Value
Simulation domain width in real space, L	50
Wave packet centre in k-space, k_0	10.0
Wave packet centre in real space, x_0	12.5
Wave packet characteristic width, σ	1.00
x-domain spacing	0.05
k-domain spacing	$\pi/25$
Time step	0.01

Table 3.1: Parameters and initial conditions for simulations of a Gaussian wave packet propagated through time using the SO method.

A simulation was performed with the same initial conditions for the numerical and analytical wave packets as those detailed in Table 3.1. It was found that both the value of $\Delta v_g(t)$ was found to be zero, and the overlap of $\psi_{\text{numerical}}(x,t)$ and

$\psi_{\text{analytical}}(x,t)$ was equal to one within at least 5×10^{-14} units, for all t. This gives indication that there is excellent agreement between the SO-propagated wave packet and the analytical result; the latter result highlights that $\psi_{\text{numerical}}(x,t)$ is in near perfect agreement with $\psi_{\text{analytical}}(x,t)$, with small discrepancies likely due to numerical noise. The remainder of the simulation results are shown in Figure 3.1a, Figure 3.1b and Figure 3.1c. These Figures demonstrate that the SO method performs extremely well when numerically propagating the Gaussian wave packet compared to the analytical result as the value of each metric is either zero ore vanishingly small. The fluctuation seen in these Figures can be attributed to numerical noise.

Whilst the overall square magnitude of the error on the propagated wave packet, it is important to acknowledge that Figure 3.1a exhibits a rough periodic trend whereby the the norm square error on the wave packet oscillates. This observation could indicate that there is some error when determining the phase velocities of the component wavefunctions of the overall wave packet. This is in contrast to the behaviour of Figure 3.1b and Figure 3.1c where, despite the numerical noise, no such oscillations exist – the noise is centred approximately on a horizontal line.

These results successfully verify that the implementation of the SO method to propagate Gaussian wave packets through time is sound, and correctly reproduces, within an acceptable error, the results of analytical quantum mechanics.

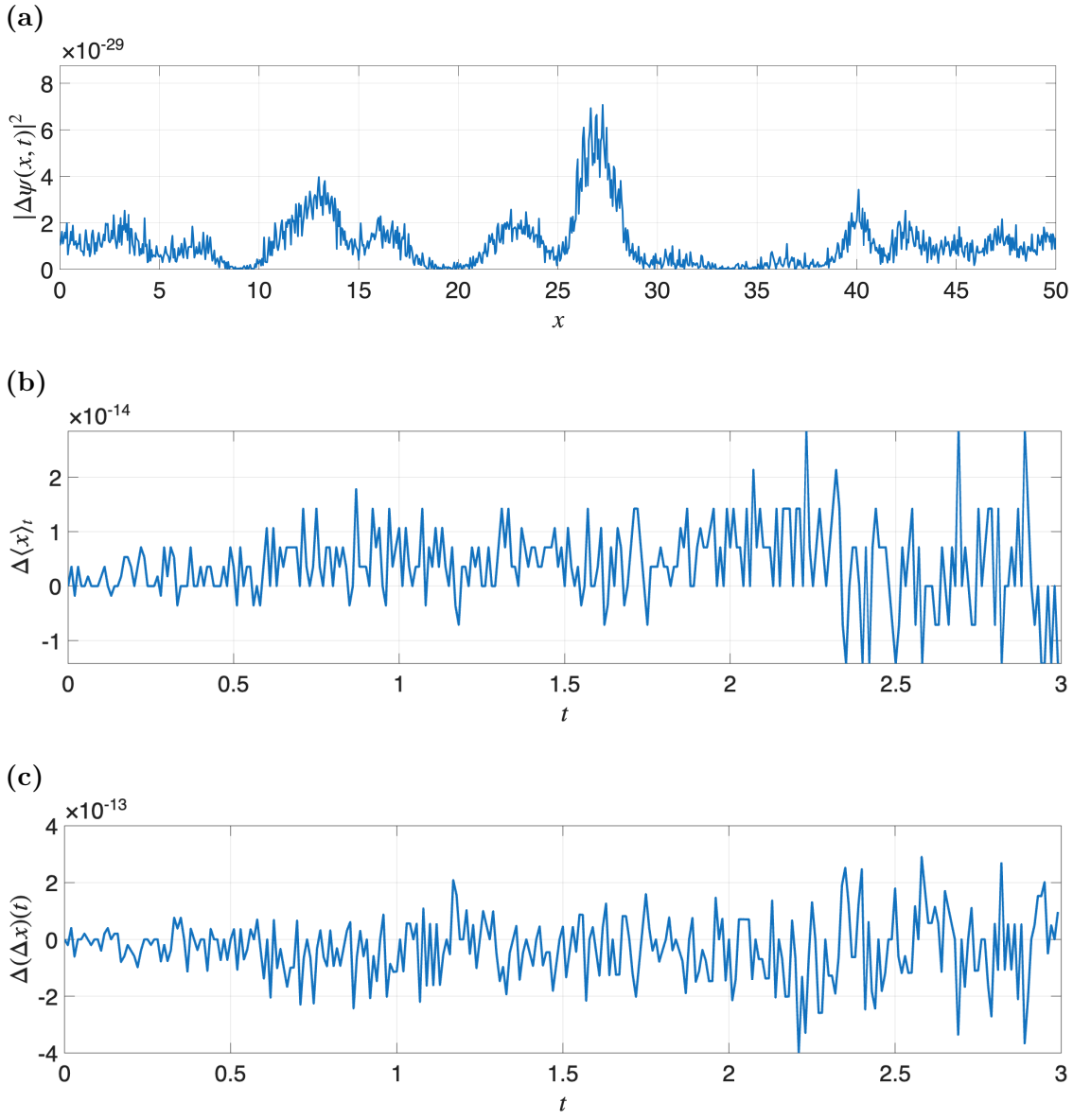

Figure 3.1: A graph of (a) the square norm of the error on the real and imaginary parts of a Gaussian wave packet propagated using the SO method versus position, x at time $t = 3.0$, (b) the error on the average position of a Gaussian wave packet propagated using the SO method versus simulation time, t, and (c) the error on the dispersion of a Gaussian wave packet propagated using the SO method versus simulation time.

4
Idealised Quantum Systems

4.1 Introduction

Before moving to free particle wave packet propagation, it would be fruitful to illustrate the behaviour of wave packets in the simplest sense, that is in the form of an eigenstate superposition for a idealised system. This allows for the critical role of wave packets in time-dependent quantum mechanics to be explored without the complication of quantum effects, such as dispersion, clouding the underlying physics.

To that end, one turns to the particle in a box describing a confined particle surrounded by infinitely high potential 'walls' as the simplest model for which wave packets can be investigated (Section 4.2). Wave packet behaviour when subjected to a harmonic potential, which is explored in Section 4.3, is the natural extension in complexity for this investigation.

4.2 The Particle in a Box

4.2.1 Eigenstates, Eigenvalues and Wave Packets

In the case of a particle confined by an infinite potential well of length L, the potential energy function is

$$V(x) = \begin{cases} 0, & 0 < x < L \\ \infty, & \text{otherwise} \end{cases}. \tag{4.1}$$

The TDSE with the particle in a box Hamiltonian is easily soluble to give the time-dependent eigenstates

$$\psi_n(x,t) = \sqrt{\frac{2}{L}} \sin\left(\frac{n\pi x}{L}\right) e^{-iE_n t/\hbar}, \tag{4.2}$$

with the corresponding eigenvalues

$$E_n = \frac{h^2 n^2}{8mL^2} \tag{4.3}$$

and wavenumbers

$$k_n = \frac{n\pi}{L}. \tag{4.4}$$

A wave packet comprised of particle in a box eigenstates with quantum numbers in the set $\mathcal{Q}$ can be generated using the principles discussed in Section 2.3 to give

$$\Psi(x,t) = \frac{1}{N} \sum_{m\in\mathcal{Q}} c_m \sin\left(\frac{m\pi x}{L}\right) e^{-iE_m t/\hbar}, \tag{4.5}$$

where c_m is an arbitrary expansion coefficient associated with $|\psi_m(x,t)\rangle$. For instance, if

$$c_m = \sqrt{\frac{2}{L}} \exp\left(-\frac{(k_m - k_0)^2}{2\sigma^2}\right), \tag{4.6}$$

then $\{c_m\}$ is a set of normally distributed coefficients. Additionally,

$$N^2 = \sum_{m\in\mathcal{Q}} |c_m|^2 \tag{4.7}$$

to ensure $\Psi(x,t)$ is normalised. In essence, the wave packet is a superposition of particle in a box eigenstates where the coefficient of each term is a Gaussian function centred on the wavenumber k_0, with a width characterised by σ.

4.2.2 Time Evolution of Particle in a Box Eigenstates

As suggested by Equation 4.2, the behaviour of time-dependent eigenstates of the particle in a box Hamiltonian is intuitive. Such states are characterised as being stationary because all the time dependence is contained in the exponential phase term, which vanishes when the norm of the wavefunction is calculated. However, the eigenstates themselves do oscillate sinusoidally in time according to the phase factor $e^{-iE_n t/\hbar}$, with a time period $T_n = \hbar/E_n$.

4.2.3 Time Evolution of Wave Packets

Non-stationary states are obtained when a wavefunction is a superposition of eigenstates, analogous to Equation 4.5. In this case, the probability flux (Equation 2.32) is non-zero, highlighting that the probability distribution is not in equilibrium, when the probability density is in motion.

Consider a wave packet comprised of q particle in a box eigenfunctions, that is $\Psi(x,t)$ with $\mathcal{Q} = \{1, 2, 3, ..., q\}$, where each term in the superposition is equally weighted. This is given by

$$\Psi_q(x,t) = \sqrt{\frac{2}{Lq^2}} \sum_{p=1}^{q} \sin\left(\frac{p\pi x}{L}\right) e^{-iE_p t/\hbar}. \tag{4.8}$$

Without loss of generality when setting $t = 0$, because $\Psi(x,0)$ is comprised solely of sine functions which are zero at $x = 0$ and $x = L$ by construction, it follows that the spatial period of Equation 4.8 is $2L$ because the ground state, ψ_1 is included in the wave packet. To verify this conclusion, one can use Lagrange's trigonometric identity to rewrite Equation 4.8 with $t = 0$ as

$$\Psi(x,0) = \sqrt{\frac{2}{LN^2}} \frac{\cos\left(\frac{\pi x}{2L}\right) - \cos\left(\frac{(q+1/2)\pi x}{L}\right)}{2\sin\left(\frac{\pi x}{2L}\right)}, \tag{4.9}$$

which has a spatial period of $2L$ and the result is thus verified.

The time period of $\Psi_q(x,t)$, $\tilde{T}_q$, can be calculated by considering the phase difference between each pair of component eigenfunctions, that is

$$\Delta\phi = \frac{(E_q - E_p)t}{\hbar}, \tag{4.10}$$

and finding the value of t for which Equation 4.10 equals $2\pi\varepsilon$ where $\varepsilon \in \mathbb{Z}$. It follows that

$$\tilde{T}_q = \frac{4\varepsilon m L^2}{\gcd(q^2 - p^2 \mid \forall\ q > p)\pi\hbar}, \tag{4.11}$$

where $\gcd(q^2 - p^2 \mid \forall\ q > p)$ is the greatest common divisor of $q^2 - p^2$ when considering all $q > p$.

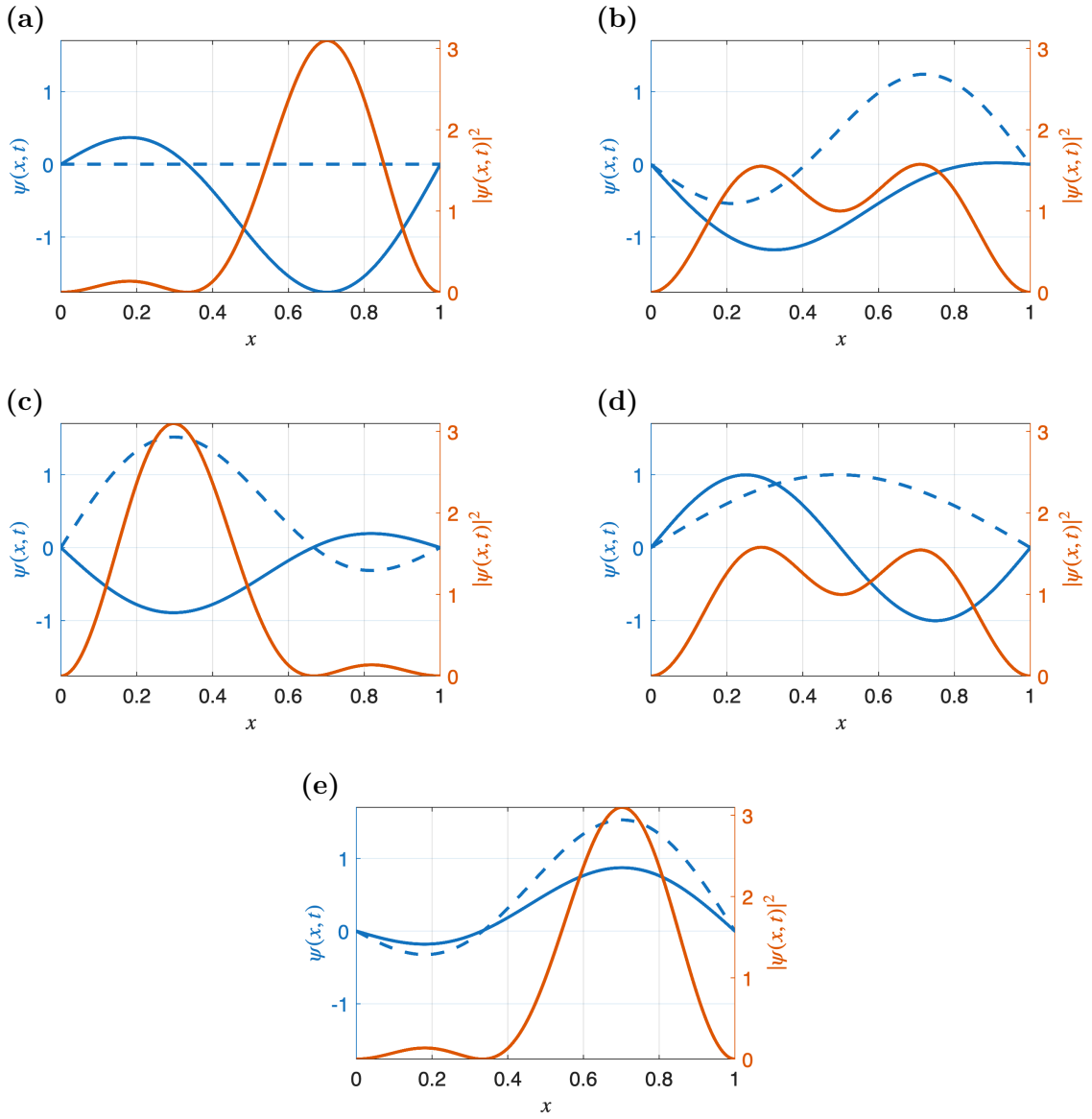

Figure 4.1: A graph of the real part (solid blue line) and imaginary part (dotted blue line) of Equation 4.12 and the corresponding probability density (orange line) at (a) $t = 0$, (b) $t = \tilde{T}_2/4$, (c) $t = \tilde{T}_2/2$, (d) $t = \tilde{3}T_2/4$, and (e) $t = \tilde{T}_2$.

Now consider the normalised two-state superposition

$$\Psi_2(x,t) = \sqrt{\frac{1}{L}}\left[\sin\left(\frac{\pi x}{L}\right)e^{-iE_1 t/\hbar} + \sin\left(\frac{2\pi x}{L}\right)e^{-iE_2 t/\hbar}\right]. \tag{4.12}$$

Using Equation 4.11, the time period of Equation 4.12 is

$$\tilde{T}_2 = \frac{4mL^2}{3\pi\hbar}; \tag{4.13}$$

Parameter	Assigned Value
Simulation domain width in real space, L	1
Spatial domain spacing	1.3335×10^{-4}
Time step	$4mL^2/(3000\pi\hbar)$

Table 4.1: Parameters and initial conditions for simulations of $\Psi(x,t)$ propagated through time using the CN method.

MATLAB scripts have been written to simulate the quantum dynamics of Ψ_2 using the CN method outlined in Section 3.1. The initial conditions of the simulation are shown in Table 4.1; natural units were adopted for simplicity, that is $\hbar = h = m = 1$. Figure 4.1 illustrates the results. The wave packet and corresponding probability density oscillate in back and forth whilst remaining zero at $x = 0$ and $x = L$. Notice that $\tilde{T}_2$ is clearly not the classical time period of the wave packet oscillation, as evidenced by the fact that Figure 4.1a is not identical to Figure 4.1e. This apparent paradox can be resolved by recognising that wavefunctions cannot be observed directly – in essence, $\tilde{T}_2$ describes the time period of the observable aspect of Ψ_2, that is the probability density which depends solely on $E_2 - E_1$ as per Equation 2.16.

As will be expanded upon later in Chapter 5, Ψ_2 does not 'travel' in the positive or negative x-direction in the same sense as a free particle wave packet. This is because the wave packet does not have any initial momentum, and dispersion is not a quantum effect seen for wave packets of the form of Equation 4.8.

4.3 The Quantum Harmonic Oscillator

4.3.1 Eigenstates, Eigenvalues and Wave Packets

The Hamiltonian for the QHO includes a quadratic potential term:

$$\hat{H} = -\frac{\hbar^2}{2m}\frac{\partial^2}{\partial x^2} + \frac{1}{2}m\omega^2\hat{x}^2, \tag{4.14}$$

where ω is the angular frequency of the harmonic oscillator. Solving the TDSE with the Hamiltonian given by Equation 4.14 allows one to recover the eigenstates of the QHO which are

$$\psi_n(x,t) = \frac{1}{\sqrt{2^n n!}}\left(\frac{m\omega}{\pi\hbar}\right)^{1/4} H_n\left(\sqrt{\frac{m\omega}{\hbar}}x\right) e^{-[m\omega x^2 - i\omega\hbar(n+1/2)t]/\hbar}, \tag{4.15}$$

where

$$H_n\left(\sqrt{\frac{m\omega}{\hbar}}x\right) = \left(\frac{\hbar}{m\omega}\right)^{n/2} (-1)^n e^{m\omega x^2/\hbar}\frac{d^n}{dx^n}e^{-m\omega x^2/\hbar} \tag{4.16}$$

are the physicist's Hermite polynomials and the energy eigenvalues are

$$E_n = \hbar\omega\left(n + \frac{1}{2}\right). \tag{4.17}$$

The set of all QHO eigenfunctions forms a discrete basis, so a wave packet constructed such eigenfunctions with quantum numbers specified in the set $\mathcal{P}$ takes the form:

$$\Psi(x,t) = \frac{1}{N}\sum_{j\in\mathcal{P}} c_j H_n\left(\sqrt{\frac{m\omega}{\hbar}}x\right) e^{-[m\omega x^2 - i\hbar\omega(j+1/2)t]/\hbar}, \tag{4.18}$$

where c_j is the expansion coefficient of $\psi_j(x,t)$ and

$$N^2 = \sum_{j\in\mathcal{P}} |c_j|^2 \tag{4.19}$$

is a normalisation constant.

4.3.2 Time Evolution of Eigenstates

Eigenstates of the QHO evolve analogously to the general solution to the TDSE obtained via the separation of variables method outlined in Section 2.1.1, that is in an oscillatory manner with a frequency of $\omega(j + 1/2)$ and time period of $[\omega(j + 1/2)]^{-1}$, where j is the quantum number of the eigenstate with energy E_j. Pure eigenstates of the QHO are stationary, so their probability densities do not oscillate with time because the complex time-dependent phase term in Equation 4.15 vanishes when its norm squared is calculated. To substantiate this, $\psi_{10}(x,t)$ and its corresponding probability density is shown in Figure 4.2.

Evidence of the correspondence principle can be seen in Figure 4.2 in that the amplitude of the probability density is highest towards the classical turning points of the harmonic oscillator. This means that the quantum particle trapped in the harmonic potential is more likely to be found at these turning points, which aligns with the conclusions of the classical dynamics of a harmonically oscillating system. The real and imaginary components will oscillate with a frequency of $2/(21\omega)$ according Equation 4.15 with $n = 10$. Note that Figure 4.2, as well as all other figures presented in this section, have been generated using MATLAB simulations run with the initial parameters presented in Table 4.2.

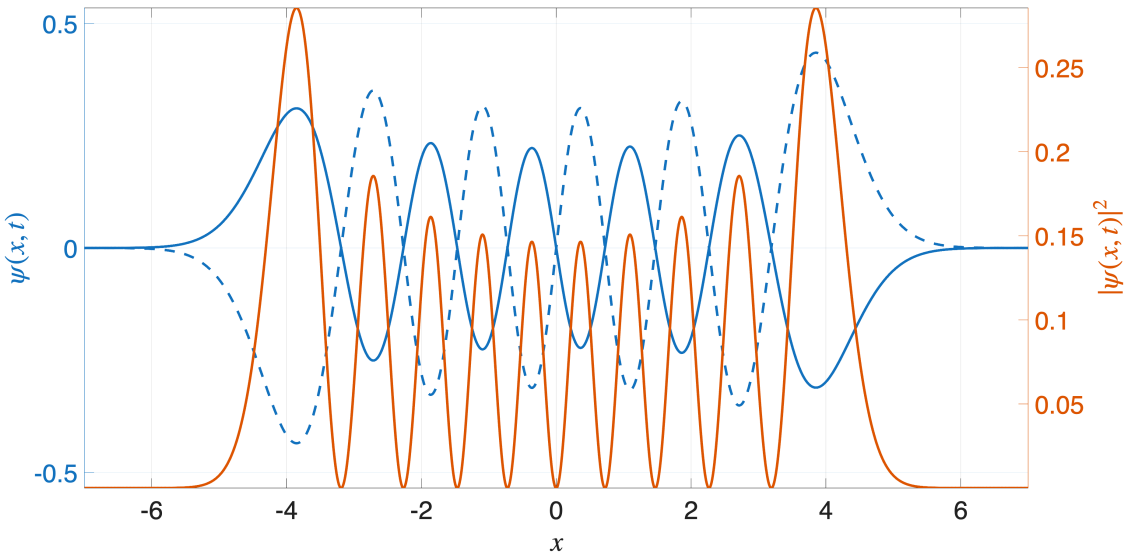

Figure 4.2: A graph of the real (blue solid line) and imaginary (blue dotted line) part of $\psi_{10}(x,t)$ and the probability density $|\psi_{10}(x,t)|^2$ (orange solid line) against position, x at time $t = 0.10$.

Parameter	Assigned Value
Angular frequency, ω	1
Simulation domain width in real space, L	20
x-domain spacing	0.002
k-domain spacing	$\pi/20$

Table 4.2: Parameters and initial conditions for simulations of a Gaussian wave packet with no net momentum propagated through time using the SO method.

4.3.3 Time Evolution of Wave Packets

Consider the normalised superposition of the first two eigenstates of the QHO:

$$\Psi(x,t) = c_0\psi_0(x,t) + c_1\psi_1(x,t), \tag{4.20}$$

where ψ_0 and ψ_1 are given by Equation 4.15 with $n = 0$ and $n = 1$, respectively, and c_1 and c_2 are constants. The probability density

$$|\Psi(x,t)|^2 = |c_0|^2|\psi(x)|^2 + |c_1|^2|\psi(x)|^2 + 2\mathrm{Re}\left[c_0^* c_1 \psi^*(x)\psi(x)e^{-i\omega t}\right] \tag{4.21}$$

clearly varies with time, and hence $\Psi(x,t)$ can be classified as a non-stationary state with a time period $T = 2\pi/\omega$.

Figure 4.3 illustrates the how the wave packet and its probability density evolve over one time period. The oscillation of the probability density indicates that the probability of finding the particle described by the wave packet at a given location on the x-axis changes with time. The oscillatory nature of this variation originates from the complex phase factor that is present in the expression for $|\Psi(x,t)|^2$.

The expectation value of position can easily be calculated by first noting that the position operator can be expressed as a sum of creation operators, $\hat{a}^\dagger$ and annihilation operators, $\hat{a}$:

$$\hat{x} = \sqrt{\frac{\hbar}{2m\omega}}\left(\hat{a}^\dagger + \hat{a}\right). \tag{4.22}$$

Thus,

$$\langle x\rangle = \sqrt{\frac{\hbar}{2m\omega}}\langle\Psi(x,t)|\left(\hat{a}^\dagger + \hat{a}\right)|\Psi(x,t)\rangle. \tag{4.23}$$

Expanding the state $|\Psi(x,t)\rangle$ and simplifying the resulting expression yields

$$\langle x\rangle = \sqrt{\frac{\hbar}{2m\omega}}\left(c_0^* c_1 e^{-i\omega t} + c_1^* c_0 e^{i\omega t}\right) \tag{4.24}$$

$$= 2\sqrt{\frac{\hbar}{2m\omega}}\mathrm{Re}\left(c_0^* c_1 e^{-i\omega t}\right) \tag{4.25}$$

$$= 2|c_0||c_1|\sqrt{\frac{\hbar}{2m\omega}}\cos\left(\omega t + \Delta\right), \tag{4.26}$$

where $c_n = |c_n|e^{i\Delta}$. Equation 4.26 demonstrates that the expectation value of position oscillates sinusoidally between $\pm 2|c_0||c_1|\sqrt{\hbar/2m\omega}$ with an angular frequency $\omega = (E_1 - E_0)/\hbar$ and shifted by the relative phase between the expansion coefficients, Δ. This contrasts with the expectation value of position for a single eigenstate of the QHO, $|\psi_n\rangle$, which is identically zero for all values of n.

DO I ADD IN A CALCULATION OF $< x^2 >$ HERE IN ORDER TO DETERMINE Delta x?

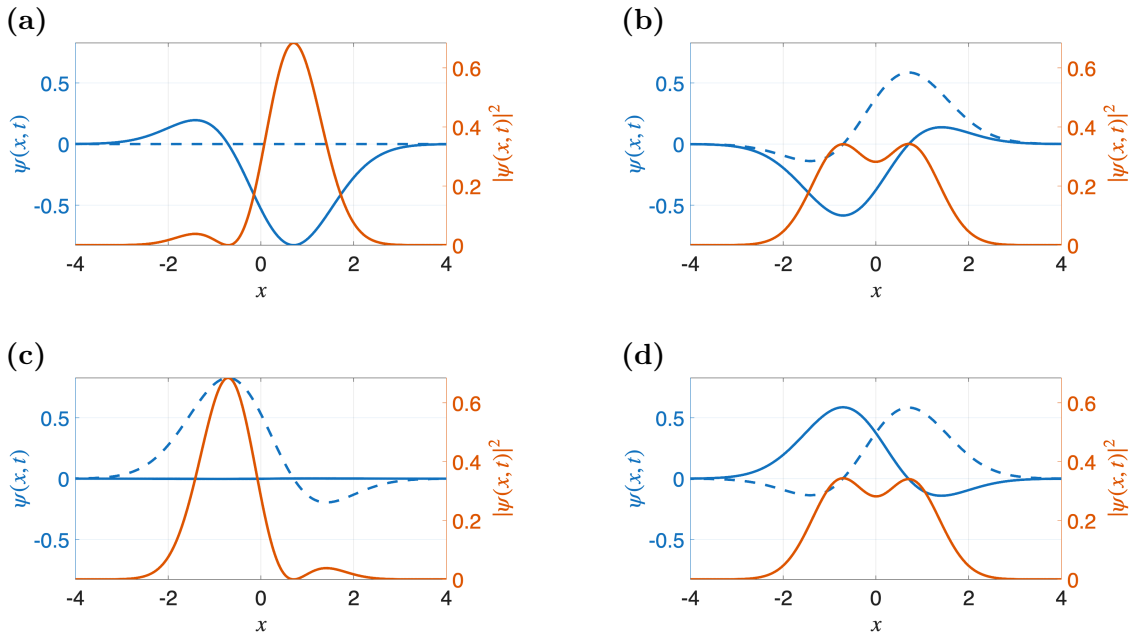

Figure 4.3: A graph of the real (blue solid line) and imaginary (blue dotted line) parts of $\Psi(x,t)$, and the probability density $|\Psi(x,t)|^2$ (orange solid line), at (a) $t = 0$, (b) $t = T/4$, (c) $t = T/2$ and (d) $t = 3T/4$.

5 Gaussian Wave Packets

5.1 Dynamics of Gaussian Wave Packets

A Gaussian wave packet in one dimension is defined as

$$\psi(x,t) = \int_{-\infty}^{\infty} e^{-(k-k_0)^2/2\sigma^2} e^{ikx}\, dk, \tag{5.1}$$

where σ and k_0 denote the standard deviation of the Gaussian function, and hence the width of the wave packet, and the initial position of the centre of the wave packet in k-space, respectively.

5.1.1 Free Particle Eigenstates

A free particle forms a system which is subjected to a constant potential that, without loss of generality, may be set to zero. As such, the wavefunction evolves according to the following TDSE:

$$\frac{\partial\psi(x,t)}{\partial t} = \frac{i\hbar}{2m}\frac{d^2\psi(x,t)}{dx^2}. \tag{5.2}$$

Employing the separation of variables method discussed in Section 2.1.1 gives the following eigenfunctions of the free particle Hamiltonian:

$$\phi_k(x,t) = e^{i(\pm kx - \hbar k^2 t/2m)}, \tag{5.3}$$

with the corresponding energy eigenvalues

$$E_k = \frac{\hbar^2 k^2}{2m}. \tag{5.4}$$

Noting that $E_k = \hbar\omega$ with ω representing an angular frequency, the dispersion relation describing how ω depends on the wavenumber can be derived. Trivial algebra reveals that

$$\omega(k) = \frac{\hbar k^2}{2m}. \tag{5.5}$$

5.1.2 General Wave Packets

The set of free particle eigenfunctions form a complete basis. Therefore, a wave packet can be formed from a superposition of elements of this basis to yield

$$\psi(x,t) = \int_{-\infty}^{\infty} a(k) e^{i(kx - \hbar k^2 t/2m)}\, dk, \tag{5.6}$$

where the function $a(k)$ is determined by evaluating

$$a(k) = \frac{1}{2\pi} \int_{-\infty}^{\infty} \psi(x,0) e^{-ikx}\, dx. \tag{5.7}$$

Equation 5.6 is essentially the inverse Fourier transform of $a(k)e^{-i\hbar k^2 t/2m}$.

The average position of a free particle wave packet, $\langle x \rangle$, can now be calculated using Equation 5.6. It is convenient to do this in k space, where $\hat{x} = i\frac{\partial}{\partial k}$, since Equation 5.6 conveniently reveals the representation of $\psi(x,t)$ in momentum space. Consequently,

$$\begin{aligned}
\langle x \rangle_t &= 2\pi i \int_{-\infty}^{\infty} a^*(k) e^{i\hbar k^2 t/2m} \frac{d}{dk} \left(a(k) e^{-i\hbar k^2 t/2m} \right)\, dk && (5.8)\\
&= 2\pi i \int_{-\infty}^{\infty} a^*(k) \left(\frac{da(k)}{dk} - \frac{i\hbar k t}{m} a(k) \right)\, dk && (5.9)\\
&= \frac{\langle p \rangle t}{m} + 2\pi \int_{-\infty}^{\infty} a^*(k) \left(i \frac{da(k)}{dk} \right)\, dk && (5.10)\\
&= \frac{\langle p \rangle t}{m} + \langle x \rangle_0 && (5.11)\\
&= v_g t + \langle x \rangle_0, && (5.12)
\end{aligned}$$

where $\langle x \rangle_0$ is the position of the centre of the wave packet at $t = 0$ and the group velocity,

$$v_g = \frac{d\langle x \rangle_t}{dt} = \frac{\langle p \rangle}{m}. \tag{5.13}$$

Note that the group velocity and average momentum is time independent which is consistent with the classical description of a free particle. Moreover, Equation 5.13 agrees with the definition of the wave packet group velocity that results when

Equation 5.5 is substituted into Equation 2.35. The phase velocity of a wave, that is the speed at which an individual wave moves, is given by

$$v_p = \frac{\omega}{k} = \frac{\hbar^2 k}{2m}. \tag{5.14}$$

As discussed in Section 2.3, the dispersion of a wave packet in real space is inversely related to the dispersion of a wave packet in momentum space. The dispersion of a wave packet, $D(t)$, is calculated using Equation 5.15:

$$D(t) = \sqrt{(\Delta x)_t^2 - (\Delta x)_0^2} \tag{5.15}$$

where

$$(\Delta x)_t^2 = \langle x^2 \rangle_t - \langle x \rangle_t^2. \tag{5.16}$$

$\langle x \rangle_t^2$ can be readily determined using Equation 5.11, so all that is left to compute is $\langle x^2 \rangle_t$, which requires solving

$$\langle x^2 \rangle_t = -2\pi \int_{-\infty}^{\infty} a^*(k) e^{i\hbar k^2 t/2m} \frac{d^2}{dk^2} \left(a(k) e^{-i\hbar k^2 t/2m} \right) \, dk. \tag{5.17}$$

Given that

$$\frac{d^2}{dk^2} \left(a(k) e^{-i\hbar k^2 t/2m} \right) = \frac{d}{dk} \left[\left(\frac{da(k)}{dk} - \frac{i\hbar k t}{m} a(k) \right) e^{i\hbar k^2 t/2m} \right] \tag{5.18}$$

$$= \left[\frac{d^2 a}{dk^2} - \frac{i\hbar t}{m} \left(\left(\frac{\hbar k t}{m} \right)^2 a(k) + a(k) + 2\frac{da}{dk} \right) \right] e^{i\hbar k^2 t/2m}, \tag{5.19}$$

and assuming $a(k)$ is real, means Equation 5.17 can be rewritten as

$$\langle x^2 \rangle_t = -2\pi \int_{-\infty}^{\infty} a(k) \left[\frac{d^2 a}{dk^2} - \frac{i\hbar t}{m} \left(\left(\frac{\hbar k t}{m} \right)^2 a(k) + a(k) + 2\frac{da}{dk} \right) \right] \, dk \tag{5.20}$$

$$= 2\pi \int_{-\infty}^{\infty} a(k) \left[\left(\frac{\hbar k t}{m} \right)^2 a(k) - \frac{d^2 a}{dk^2} \right] \, dk. \tag{5.21}$$

The progression from Equation 5.20 to Equation 5.21 recognises that

$$2 \int_{-\infty}^{\infty} a \frac{da}{dk} \, dk = \int_{-\infty}^{\infty} (a(k))^2 \, dk. \tag{5.22}$$

The assumption that $a(k)$ is real implies $\langle x \rangle_0 = 0$ because Equation 5.10 is an integral over a symmetric interval with an integrand that is an odd function of k. It also guarantees that the wave packet is maximally compact at $t = 0$. It now follows that

$$[D(t)]^2 = 2\pi \int_{-\infty}^{\infty} \left(\frac{\hbar k t}{m} \right)^2 |a(k)|^2 \, dk - \left(\frac{\hbar \langle k \rangle t}{m} \right)^2 \tag{5.23}$$

which simplifies to

$$D(t) = \frac{\hbar \Delta k}{m} t, \tag{5.24}$$

where $\Delta k = \sqrt{\langle k^2 \rangle - \langle k \rangle^2}$ is the uncertainty in the wavenumber.

5.2 Gaussian Wave Packets within a Constant Potential

5.2.1 Time Propagation with No Net Momentum

Wave packets without any net momentum and subjected to a constant potential have an expectation value of zero for k, hence its group velocity is also zero; Equation 5.1 with k_0 set to zero, that is

$$\psi_{\text{stat}}(x,t) = \int_{-\infty}^{\infty} e^{-k^2/2\sigma^2} e^{ikx}\, dk, \tag{5.25}$$

describes such a system. This specific case allows for the phenomenon of dispersion, as defined by Equation 5.25, to studied in isolation.

Parameter	Assigned Value
Simulation domain width in real space, L	50
Wave packet centre in k-space, k_0	0.0
Wave packet centre in real space, x_0	25
Wave packet characteristic width, σ	1.0
Spatial domain spacing	0.050
k-spacing	$\pi/25$
Time step	0.01

Table 5.1: Parameters and initial conditions for simulations of a Gaussian wave packet with no net momentum propagated through time using the SO method.

MATLAB simulations were written to graphically illustrate dispersion effects on Gaussian wave packets with no net momentum. Figure 5.1 shows the time evolution of the real and imaginary parts of the Gaussian wave packet. It is evident that as time progresses, the centre of the wave packet remains fixed at $x = 0$, but its width increases. Furthermore, the imaginary part becomes non-zero due to the complex phase factor contained in the time evolution operator. The reason dispersion occurs is because the wave packet is formed from a superposition of plane waves that each have different spatial frequencies that are normally distributed about $k = 0$ (hence why the group velocity is zero). Consequently, each component is moving with a different phase velocity causing the wave packet to spread out in space.

One consequence of wave packet spreading is that its probability density must also disperse over time. Of course, this makes sense from a purely mathematical argument in that the probability density is given by $|\psi_{\text{stat}}(x,t)|^2$, so if the Gaussian envelope of $\psi_{\text{stat}}(x,t)$ widens in space, so must its probability density. However, a more physically motivated explanation is that probability must be conserved, so if the

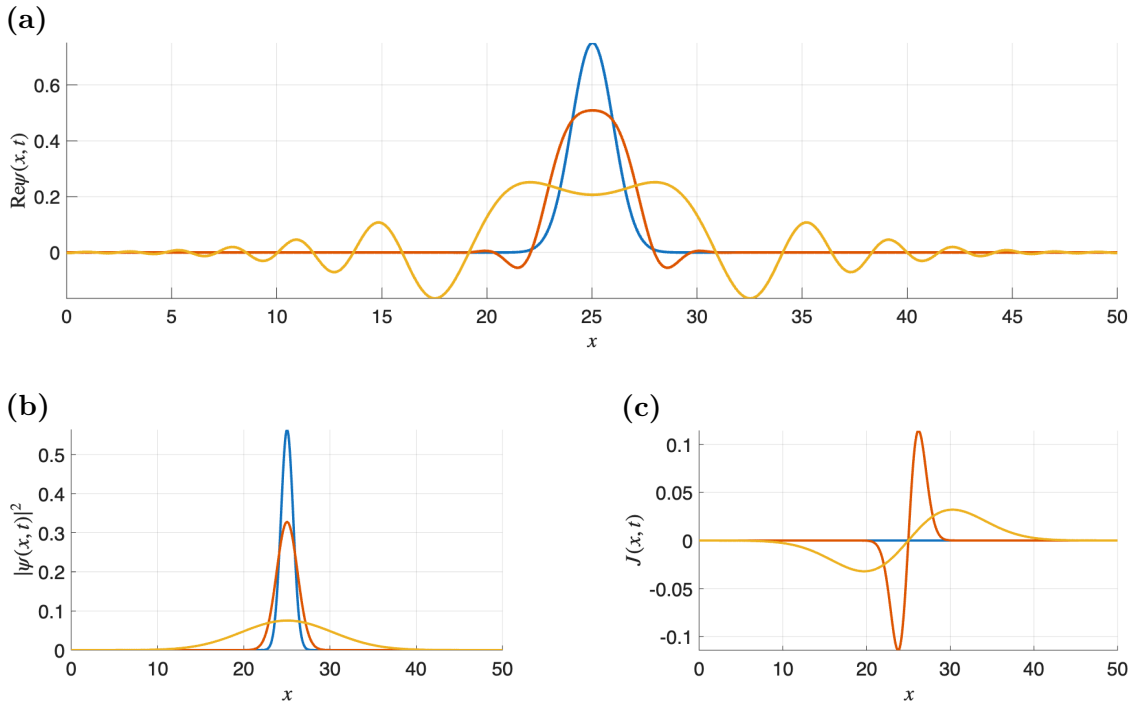

Figure 5.1: A graph at time $t = 0$, $t = 2.4$ and $t = 7.4$ of (a) the real part of a Gaussian wave packet with a net momentum of $k = 10$, (b) its corresponding probability, and (c) the flux.

amplitude of the wave packet decreases, then the probability density must broaden to account for this loss of amplitude and conserve probability. One may draw parallels between the one-dimensional diffusion equation with diffusion coefficient D given by

$$\frac{\partial y(x,t)}{\partial t} = D\frac{\partial^2 y(x,t)}{\partial x^2}, \tag{5.26}$$

and the TDSE with the potential set to zero (reproduced here for convenience):

$$\frac{\partial \psi_{\text{stat}}(x,t)}{\partial t} = \frac{i\hbar^2}{2m}\frac{\partial^2 \psi_{\text{stat}}(x,t)}{\partial x^2}, \tag{5.27}$$

to rationalise the diffusion behaviour of the wave packet in Figure 5.1 and Figure 5.1b.

Finally, because the probability density morphs over time, there must be a non-zero probability flux for all $t > 0$, and indeed this is borne out in Figure 5.1c which shows an odd flux function about $x = 25$, the centre of the wave packet. An odd function is seen for flux because of the symmetric distribution of k-values that the free particle eigenfunctions comprising the wave packet possess, thus causing the wave packet to disperse symmetrically about its centre. As is to be expected, the amplitude of J decreases over time as the spatial extent of which the wave packet, and hence the probability density, increases over time.

5.2.2 Time Propagation with Net Momentum

MATLAB scripts have also been written to simulate the dynamics of a Gaussian wave packet with a net momentum over time using the SO method. The initial conditions for the wave packet are presented in Table 5.2 and Figure 5.2 shows the state of the wave packet at the beginning of the simulation. The flux is calculated using Equation 2.32. Note that only the real part of the Gaussian wave packet is shown in Figure 5.2 for clarity; the imaginary part of the wave packet behaves analogously with the only difference being that it is offset by a small phase.

Parameter	Assigned Value
Simulation domain width in real space, L	50
Wave packet centre in k-space, k_0	10.0
Wave packet centre in real space, x_0	12.5
Wave packet characteristic width, σ	1.00
x-domain spacing	0.05
k-domain spacing	$\pi/25$
Time step	0.01

Table 5.2: Parameters and initial conditions for simulations of a Gaussian wave packet propagated through time using the SO method.

Figure 5.2 clearly shows that the wave packet becomes broader in space as time progresses in agreement with Equation 5.24. As a consequence, both the probability density and flux increase in width and decrease in amplitude, the reasons for which are discussed in Section 5.2.1, whilst continuing to move at a constant rate equal to the group velocity of the wave packet. The wave packet, probability density and flux, shown in Figure 5.2b and Figure 5.2c, respectively, each retain the form of a Gaussian function for all time, providing there are no interactions with external potential features and that the wave packet does not interfere with itself due to numerical noise or any boundary conditions imposed on the MATLAB simulations.

An important subtlety to acknowledge is that Δk remains constant in time for a Gaussian wave packet because the square norm of the integrand in Equation 5.1 is time independent. Therefore, one may reasonably ask:

'If a travelling wave packet disperses in real space over time, why does it not disperse in momentum space?'

The crux of the answer to this question lies in the fact that because there is a non-zero value of Δk, the waves comprising the Gaussian wave packet each have a different phase velocity, so each one travels a different distance relative to all others

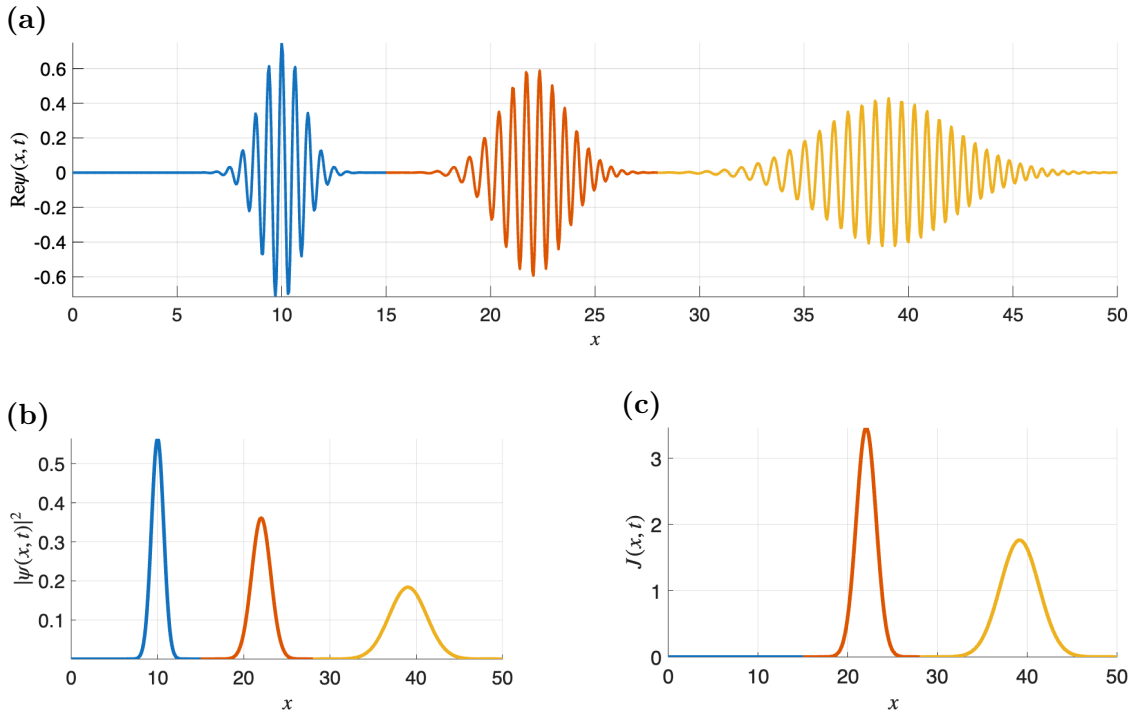

Figure 5.2: A graph at time $t = 0$ (blue line), $t = 1.2$ (orange line) and $t = 2.9$ (yellow line) of (a) the real part of a Gaussian wave packet with a net momentum of $k = 10$, (b) its corresponding probability, and (c) the flux.

in a given unit of time. Thus, the wave packet disperses equally in the positive and negative x-direction. However, after calculating the following expectation values:

$$\langle k \rangle = \frac{\sigma}{\sqrt{\pi}} \int_{-\infty}^{\infty} k e^{-(k-k_0)^2/\sigma^2} \, dk = k_0 \tag{5.28}$$

$$\langle k^2 \rangle = \frac{\sigma}{\sqrt{\pi}} \int_{-\infty}^{\infty} k^2 e^{-(k-k_0)^2/\sigma^2} \, dk = k_0^2 + \frac{\sigma^2}{2} \tag{5.29}$$

it follows that

$$\Delta k^2 = \langle k^2 \rangle - \langle k \rangle^2 = \frac{\sigma^2}{2}. \tag{5.30}$$

Therefore, because the spread of k-values that comprise the wave packet is fixed, its width remains fixed in momentum space for all time. In addition, considering the above result showing that $\langle k \rangle$ is constant in time in conjunction with the form of Equation 5.13, the group velocity is also constant. Crucially, this does not violate the Heisenberg uncertainty principle (Equation 2.37) as an increasing value Δx with a constant value of Δk only moves the wave packet further away from the minimal uncertainty state as time progresses.

5.3 Interference Between Gaussian Wave Packets

When treating systems comprised of multiple species, it it necessary to consider the constructive and destructive overlap between wavefunctions. Intuitively, such interference behaves in the same way as that between classical waves. Whether or not constructive or destructive interference is observed when wavefunctions overlap will depend on the relative phase between the interacting wavefunctions.

Wavefunction interaction is key to understanding many phenomena seen in chemical physics. Firstly, if one is to understand predict the transfer of electrons during a chemical reaction, the wavefunction overlap must be considered. Secondly, scattering processes are key to rationalising observations in spectroscopy when characterising a molecule, and wave packets play a key role in this endeavour.

5.3.1 Analysis of Wave Packet Interference

MATLAB scripts have been developed to simulate the interference patterns that manifest when two travelling Gaussian wave packets are propagated towards each other with opposite group velocity directions. Whilst in reality one should consider the two wave packets as being part of the same overall wavefunction, it aids intuition to consider them as two wave packets defined as

$$\psi_A(x,t) = \int_{-\infty}^{\infty} e^{-(k-k_0^A)^2/2\sigma^2 - x_0^A k - iEt/\hbar} e^{-ikx}\, dk \tag{5.31}$$

and

$$\psi_B(x,t) = \int_{-\infty}^{\infty} e^{-(k-k_0^A)^2/2\sigma^2 - x_0^B k - iEt/\hbar} e^{-ikx}\, dk. \tag{5.32}$$

The results of the simulation showing the wave packets propagating at representative times are illustrated in Figure 5.3, and the parameters and initial conditions pertaining to the simulation are given in Table 5.3.

Figure 5.3a shows the initial state of the system at time $t = 0$, where two identical Gaussian wave packets with group velocities equal in magnitude, but opposite in direction, are set travelling towards each other. As time progresses, the dispersion processes discussed earlier for single Gaussian wave packets are still prevalent and the wave packets disperse as usual. When the wave packets meet, they can either interfere constructively, where the amplitude of the wave packet increases, or destructively, where the amplitude of the wave packet decreases, to generate the interference patterns shown in Figure 5.3b and Figure 5.3c. When the two wave packets meet each other, the interference relationships between individual component free-particle wavefunctions will each be unique, due to the differing

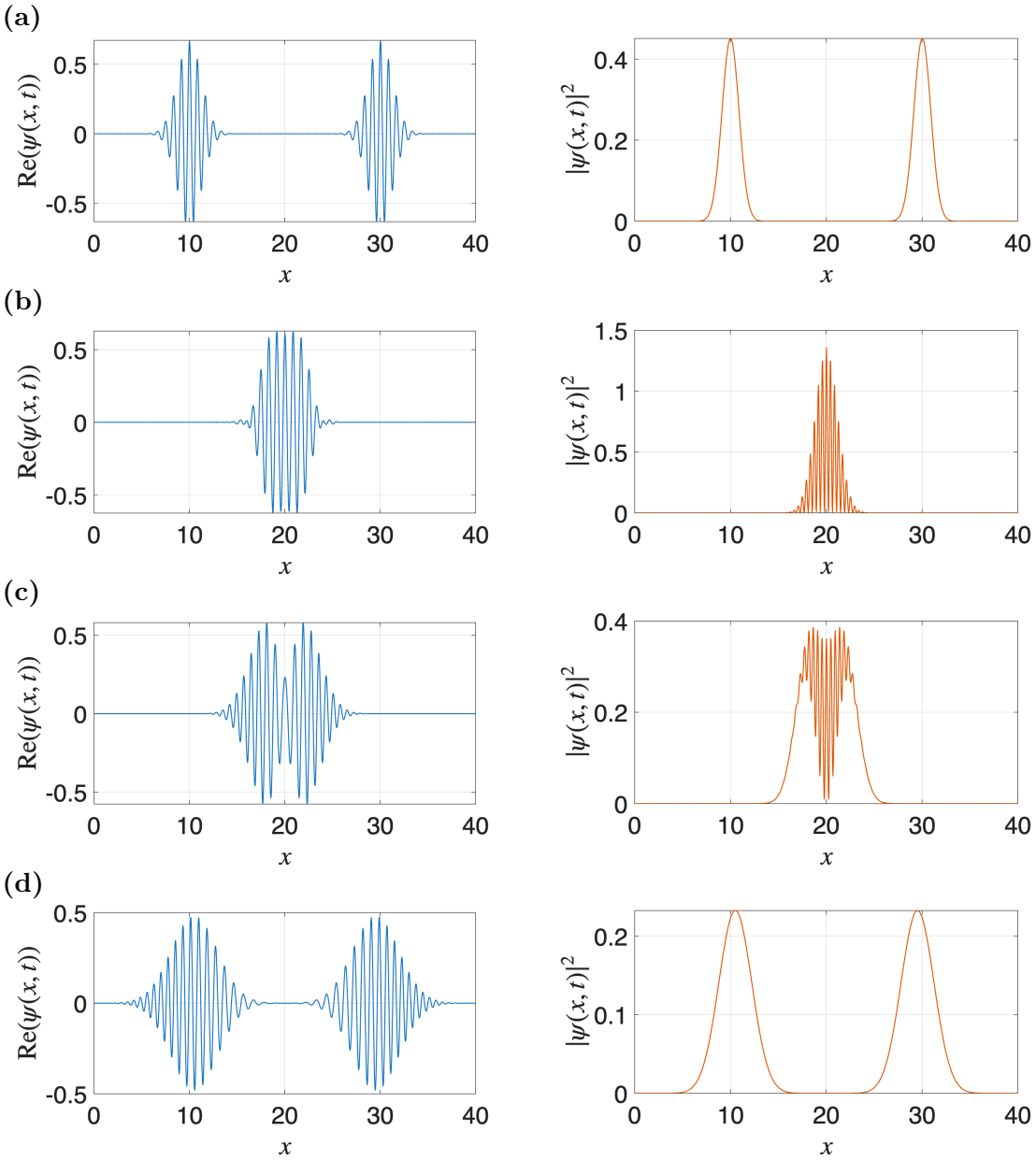

Figure 5.3: A graph of the real part of the wavefunction of two interacting Gaussians propagated through time $\psi(x,t)$ (blue line) and its corresponding probability density $|\psi(x,t)|^2$ (orange line), at (a) $t = 0$, (b) $t = 1.35$, (c) $t = 1.6$ and (d) $t = 2.6$.

Parameter	Assigned Value
Simulation domain width in real space, L	40
Centre of wave packet A centre in k-space, k_0^A	7.5
Centre of wave packet B centre in k-space, k_0^B	-7.5
Centre of wave packet A centre in real space, x_0^A	10.0
Centre of wave packet B centre in real space, x_0^B	30.0
x-domain spacing	0.04
k-domain spacing	$\pi/20$
Time step	0.01

Table 5.3: Parameters and initial conditions for simulations of two interacting Gaussian wave packets propagated through time using the SO method.

relative phases between them. This gives rise to the oscillating probability densities shown in Figure 5.3a and Figure 5.3d, which can be contrasted with the simple Gaussian envelopes in Figure 5.2b. During the period of interaction, ψ_A and ψ_B may still be considered to be independently progressing with a group velocity of $k_0^A\hbar^2/2m$ and $k_0^B\hbar^2/2m$, respectively, and there is evidence of each wave packet reappearing in Figure 5.3c as the spatial overlap between them reduces. Once the spatial overlap approaches zero in Figure 5.3d, the two initial wave packets reappear with a higher degree of dispersion than at $t = 0$. The implication is that dispersion is a phenomenon which is still present even when wave packets have interacted.

5.4 Scattering and Tunnelling

A somewhat counter-intuitive, yet easily visualisable consequence of quantum mechanics is the phenomena of quantum scattering, where a wavefunction can scatter off a potential energy incline propagating it in the opposite direction, and quantum tunnelling, where a wavefunction describing a particle has a non-zero probability of being found in a classically forbidden region. One model system which exemplifies these concepts is the potential barrier, and this will be explored in this Section.

5.4.1 The Potential Barrier

Consider a system where a Gaussian wave packet of the form of Equation 5.1 is propagated through time and subjected to a potential given by

$$V(x) = \begin{cases} V_{\text{barrier}}, & x^b_{\text{lower}} \leq x \leq x^b_{\text{upper}} \\ 0, & \text{otherwise} \end{cases}, \tag{5.33}$$

where x^b_{lower} and x^b_{upper} are the lower and upper boundaries of the barrier in the x-domain, respectively, and V_{barrier} is the energy of the barrier. A MATLAB simulation

was run to investigate the scattering and tunnelling of a Gaussian wave packet when incident on the potential barrier. The initial conditions described in Table 5.4 and the wave packet is of the form of Equation 5.1.

Parameter	Assigned Value
Simulation domain width in real space, L	100
Wave packet energy, E_{WP}	25.0
Initial wave packet centre in real space, x_0	45.0
Wave packet characteristic width, σ	2.00
Barrier energy, V_{barrier}	31.25
Barrier width	0.33
x-domain spacing	0.0033
k-domain spacing	$\pi/50$
Time step	1×10^{-3}

Table 5.4: Parameters and initial conditions for the simulation of a Gaussian wave packet incident on a potential barrier propagated through time using the SO method.

Figure 5.4 shows how the wave packet evolves in time as it propagates towards, through and away from the potential barrier. Classically, because $E_{WP} < V_{\text{barrier}}$, the wave packet should be fully reflected off the barrier in the negative x-direction. However, Figure 5.4b gives clear evidence of quantum tunnelling as wave packet penetrates through the potential barrier. The wave packet continues to propagate into the classically forbidden region as time progresses, as shown by Figure 5.4c. Although the flux of the wave packet in this region is zero in agreement with the classical scenario, there is still a non-zero probability of finding the particle described by the wave packet in the classically forbidden region.

There is evidence of scattering processes in Figure 5.4b and Figure 5.4c, whereby the wave packet is partially reflected off the barrier, which is to be expected. The amplitude of the reflected wave, which travels with the same group velocity as the the incident wave and the one that has tunnelled through the barrier, is less than that of the tunnelling, wave meaning there is a greater probability of finding the particle described by the wave packet on the left hand side of the barrier compared to the right hand side.

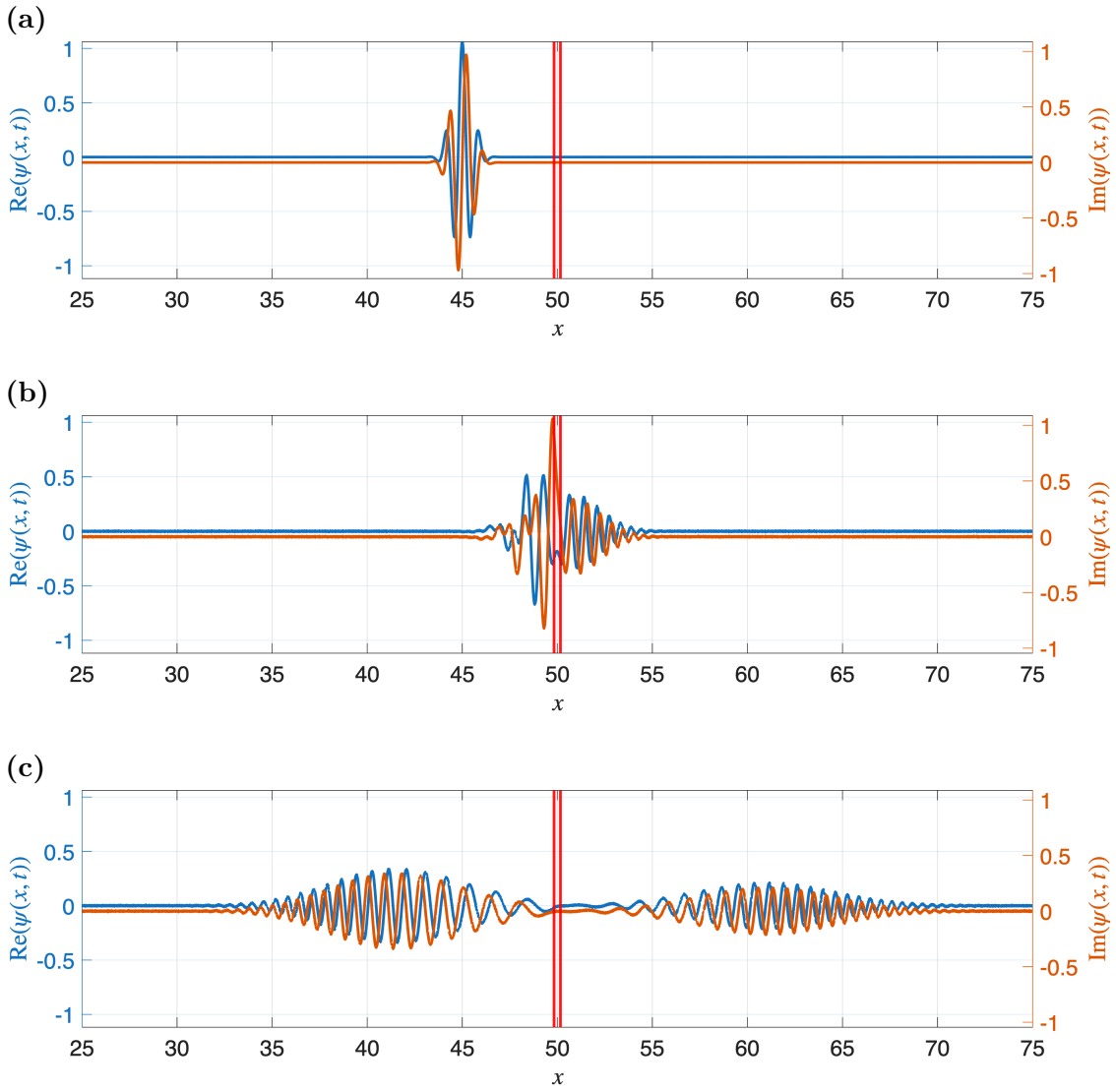

Figure 5.4: A graph of the real (blue line) and imaginary (orange line) parts of a Gaussian wave packet incident on a potential barrier, with the initial conditions given in Table 5.4, at time (a) $t = 0$, (b) $t = 0.75$, and (c) $t = 2.0$. The red vertical lines define the potential barrier with energy V_{barrier}.

6
Wave Packet Manipulation

6.1 Motivation

Whilst wave packet dynamics discussed in Chapter 5 are incredibly useful to understand the evolution of isolated quantum systems, one is often required to go further when investigating systems that interact or are subjected to a perturbation. One example that is ubiquitous throughout chemistry is the interaction between radiation and matter, the theory of which forms the cornerstone of spectroscopy and a host of other commonly used analytical techniques.

Having the ability to manipulate wave packets is useful when the behaviour of a wavefunction needs to be controlled with a high degree of accuracy. Chirping is one method which allows this. The theory of chirping can be exploited to focus a wave packet on a particular location at a particular time, say on a potential energy surface, and modify its shape. Another application is when describing the response of a wave packet to a pulse of light which excites it to a higher energy state. Chirping can also be applied to the case where one wishes to excite selected molecular vibrational modes, which may offer insight into the behaviour of the molecule at a transition state.

6.2 Chirps With a Polynomial Phase

6.2.1 Introduction

In essence, chirping involves multiplying a wave packet by a complex phase term to alter its shape how it evolves over time. The chirped wave packet may be defined in terms of an angular frequency (that is, energy space) or in momentum space. Note that the order of the chirp, for example linear or quadratic chirp, originates from the definition in the time domain, that is the inverse Fourier transform of a chirped wave packet defined in energy space. The dispersion relation (Equation 5.5) is a convenient way to transform between the energy domain and k-domain.

A Gaussian wave packet chirped with a complex polynomial phase term is given by

$$\psi_m(x,t) = \frac{1}{\sqrt{N_m}} \int_{-\infty}^{\infty} e^{-(k-k_0)^2/2\sigma^2 + i[\phi_m(k) - E(k)t/\hbar]} e^{ikx}\, dk, \tag{6.1}$$

where N_m is a normalisation constant, $E(k)$ is the energy of the state as a function of k, σ defines the width of the Gaussian envelope, and

$$\phi_m(k) = \sum_{n=1}^{m} a_n k^n \tag{6.2}$$

is a time-independent polynomial of order m.

When investigating the impact of polynomial phases given by $\phi_m(k)$ on the dispersion behaviour of a wave packet, one may calculate the time at which the dispersion is at a minimum,

$$t_{\text{disp}} = \frac{m}{\hbar \Delta k^2} \sum_{n=1}^{m} n a_n \left(\langle k^n \rangle - \langle k \rangle \langle k^{n-1} \rangle \right), \tag{6.3}$$

the position of the wave packet at time $t = 0$,

$$\langle x \rangle_0 = -\sum_{n=1}^{m} n a_n \left\langle k^{n-1} \right\rangle, \tag{6.4}$$

or the position of the wave packet at time $t = t_{\text{disp}}$,

$$\langle x \rangle_{t_{\text{disp}}} = v_g t_{\text{disp}} + \langle x \rangle_0 . \tag{6.5}$$

REFERENCE ADAM'S NOTES HERE

To aid the physical interpretation of chirped wave packets, a wave packet without any chirp imposed upon it is simply

$$\psi(x,t) = \frac{1}{\sqrt{N}} \int_{-\infty}^{\infty} e^{-(k-k_0)^2/2\sigma^2 - iEt/\hbar} e^{ikx}\, dk \tag{6.6}$$

$$= \frac{\sigma}{\sqrt{N}} e^{-\sigma^2 x^2/2 - i[k_0 x + Et/\hbar]}, \tag{6.7}$$

where N is a normalisation constant.

6.2.2 Linear Phase

Consider the case where $m = 1$ such that $\phi_m(k) = a_1 k$ and the corresponding angular frequency, $\phi(\omega) \propto \sqrt{\omega}$, leading to a wave packet with a radical chirp, $\psi_1(x,t)$:

$$\psi_1(x) = \frac{1}{\sqrt{N_1}} \int_{-\infty}^{\infty} e^{-(k-k_0)^2/2\sigma^2 + i a_1 k} e^{ikx}\, dk. \tag{6.8}$$

Hence, the time-dependent wave packet is

$$\psi_1(x,t) = \frac{\sigma}{\sqrt{N_1}} e^{-\sigma^2(x+a_1)^2/2 - i[k_0(x+a_1) + Et/\hbar]}. \tag{6.9}$$

By comparing Equation 6.7 and Equation 6.9, it follows that a radical chirp with $\phi(\omega) \propto \sqrt{\omega}$ corresponds to a shift in position by a_1 units in the negative x-direction. Furthermore, the form of Equation 6.9 indicates that its dispersion characteristics are identical to that of the unchirped Gaussian wave packet (Equation 6.7), as investigated in Chapter 4, because it is immediately clear that $\langle k \rangle = k_0$ meaning the group velocities are the same, as are the phase velocities of each component wavefunction based on Equation 2.36. Only the initial position of the wave packet is altered by the chirp.

A MATLAB script has been developed to propagate Equation 6.9 through time using the split operator method; the parameters set for the simulation are summarised in Table 6.1. Figure 6.1 clearly shows the wave packet beginning the simulation offset from the origin at $x = -15$, as expected by the coefficient a_1 in the linear phase chirp. As time progresses, the wave packet disperses according to the dispersion relation given by Equation 5.15, that is in the same fashion as an unchirped wave packet, which is evident from Figure 6.1 and the analytical derivation of Equation 6.9.

Parameter	Assigned Value
Simulation domain width in real space, L	50
Wave packet centre in k-space, k_0	10.0
Wave packet characteristic width, σ	1.00
Chirp coefficient in k-space, a_1	50/3
x-domain spacing	0.05
k-domain spacing	$\pi/25$
Time step	0.01

Table 6.1: Parameters and initial conditions for simulations of a Gaussian wave packet chirped with a linear phase in k-space propagated through time using the SO method.

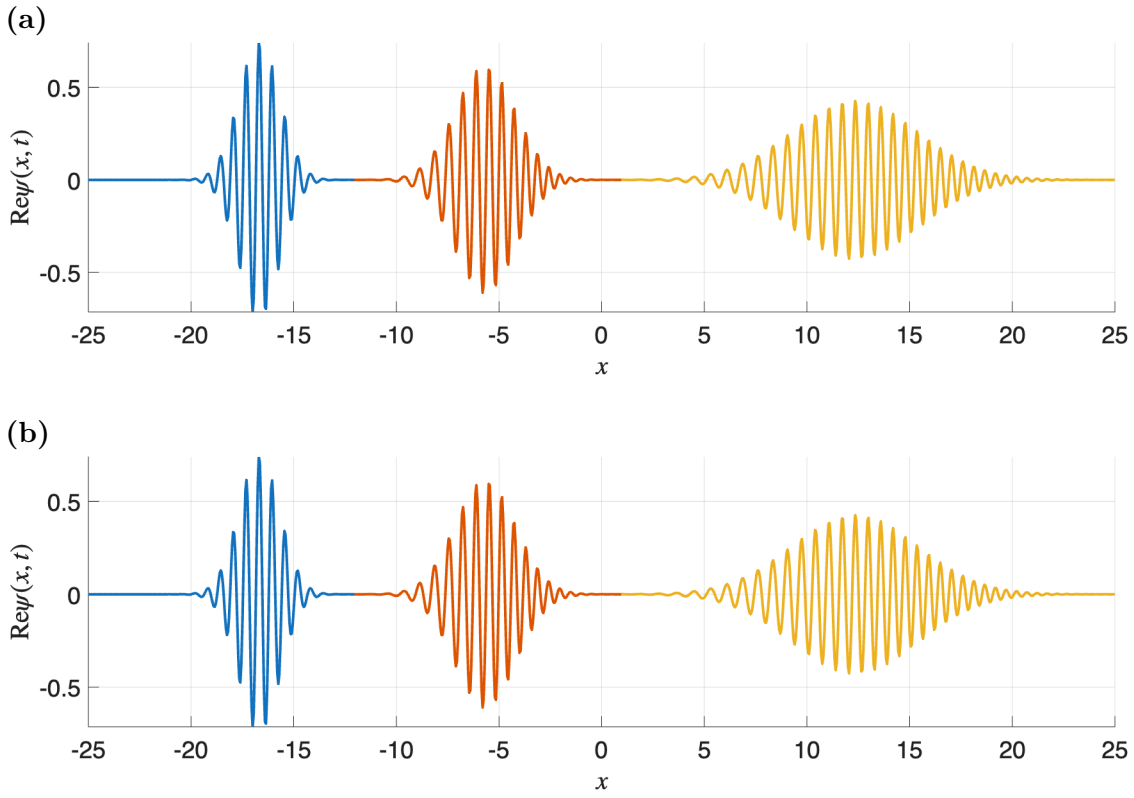

Figure 6.1: A graph at time $t = 0$ (blue line), $t = 1.1$ (orange line) and $t = 2.9$ (yellow line) of (a) the real part and (b) the imaginary part, of a Gaussian wave packet Gaussian wave packet chirped by a linear phase; the wave packet is given by Equation 6.9 with the initial conditions as specified in Table 6.1.

6.2.3 Quadratic Phase

A quadratic phase corresponds to the case where $\phi_2(k) = a_2k^2$ meaning that in energy space $\phi(\omega) \propto \omega$, thus corresponding to a linear chirp. The wave packet can therefore be written as

$$\psi_2(x) = \frac{1}{\sqrt{N_2}} \int_{-\infty}^{\infty} e^{-(k-k_0)^2/2\sigma^2 + ia_2k^2} e^{ikx}\, dk. \tag{6.10}$$

Calculating the integral of Equation 6.10, simplifying the exponent and multiplying the result by the time-evolution operator, yields the time-dependent chirped wave packet

$$\psi_2(x,t) = \frac{\exp\left[-\frac{2\sigma^2(x+2a_2k_0)^2 - 4i\left(k_0x + a_2k_0^2 - a_2\sigma^4x^2\right)}{4a_2\sigma^2+2i} - \frac{iEt}{\hbar}\right]}{\sqrt{N_2(\sigma^{-2} - 2a_2i)}}. \tag{6.11}$$

It follows that linear chirp corresponds to a time shift of the wave packet. This means that the wave packet is not maximally compact at time $t = 0$, rather Equation 6.3

can be used to show that the time at which the wave packet is maximally compact is

$$t_{\text{disp}} = \frac{2a_2 m}{\hbar \Delta k^2} \left(\left\langle k^2 \right\rangle - \langle k \rangle^2 \right) \tag{6.12}$$

$$= \frac{2a_2 m}{\hbar \Delta k^2} \left(\Delta k^2 \right) \tag{6.13}$$

$$= \frac{2a_2 m}{\hbar}. \tag{6.14}$$

It follows that the time displacement is proportional to the coefficient of k^2 in the quadratic chirp phase. The wave packet is maximally compact at the position $x = 0$, which can be shown by first calculating $\langle x \rangle_0$ using Equation 6.4 to yield

$$\langle x \rangle_0 = -2a_2 \langle k \rangle \tag{6.15}$$

$$= -\frac{2a_2 m v_g}{\hbar} \tag{6.16}$$

$$= -v_g t_{\text{disp}} \ , \tag{6.17}$$

and then trivially

$$\langle x \rangle_{t_{\text{disp}}} = v_g t_{\text{disp}} + \langle x \rangle_0 = 0. \tag{6.18}$$

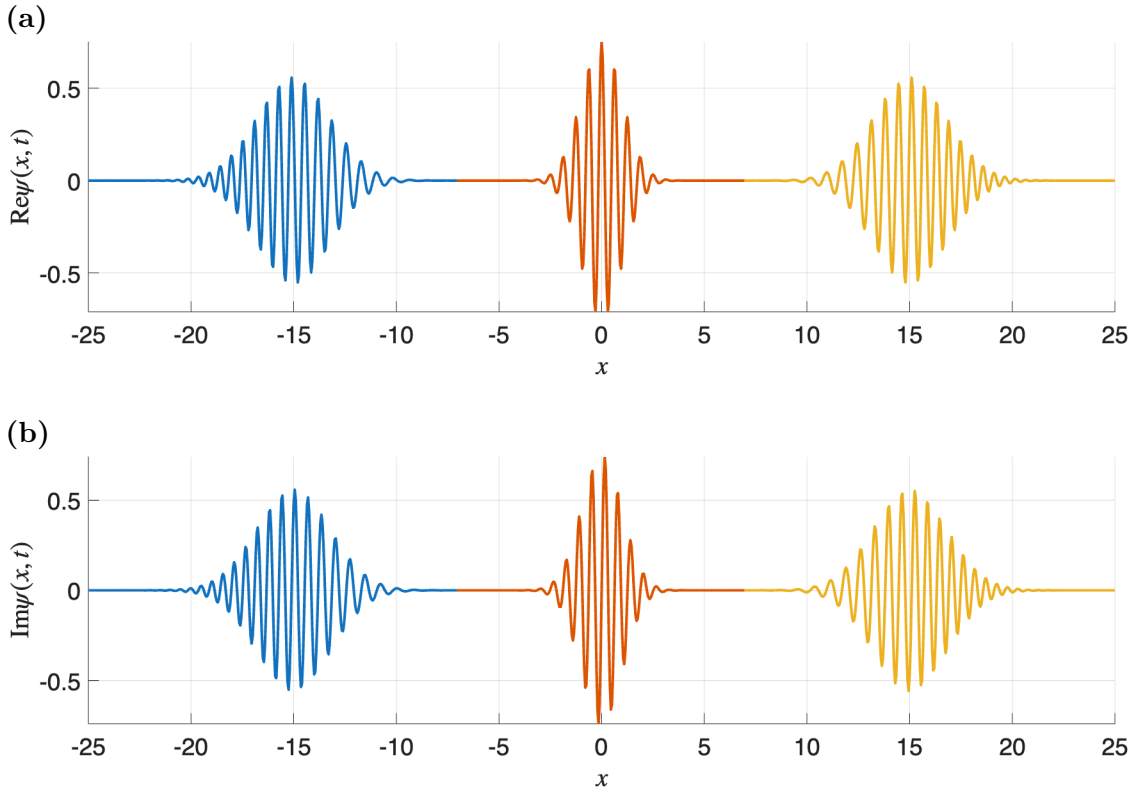

Figure 6.2: A graph at time $t = 0$ (blue line), $t = 1.50$ (orange line) and $t = 3.00$ (yellow line) of (a) the real part and (b) the imaginary part, of a Gaussian wave packet chirped by a quadratic phase; the wave packet is given by Equation 6.11 with the initial conditions as specified in Table 6.2.

Parameter	Assigned Value
Simulation domain width in real space, L	50
Wave packet centre in k-space, k_0	10.0
Wave packet characteristic width, σ	1.00
Chirp coefficient in k-space, a_2	1.50
x-domain spacing	0.05
k-domain spacing	$\pi/25$
Time step	0.01

Table 6.2: Parameters and initial conditions for simulations of a Gaussian wave packet chirped with a quadratic phase in k-space propagated through time using the SO method.

Figure 6.2 demonstrates how a Gaussian wave packet behaves when chirped with the quadratic phase $e^{-ia_2k^2}$, where $a_2 = 1.5$. At $t = 0$, the wave packet is displaced from $x = 0$ because it has been propagated into 'negative' time at $t = -1.5$. Consequently, the Gaussian wave packet begins at a negative position due to the fact that it is initiated with a positive mean k-value of 10, so its group velocity is in the positive x-direction; it also has a higher degree of dispersion. As the wave packet is evolved in time, the extent of dispersion reduces as it approaches $x = 0$ where it becomes maximally compact which in turn verifies Equation 6.14 and Equation 6.18. Once the wave packet passes the point of minimum dispersion, it propagates in the same way as an unchirped wave packet centred at the origin at $t = 0$: it disperses according to Equation 5.5 and Equation 5.24, and moves with a constant group velocity, $v_g = \hbar^2 k_0/2m$. Note from Figure 6.2 that the wave packet is symmetrical in time about $x = 0$.

7
Conclusions

Wave packet dynamics have far reaching applications in the field of chemical physics and are invaluable when wishing to probe the time-dependence of quantum systems. In Chapter 1, the motivation for developing the theory of wave packets, including why one may want to manipulate their behaviour, was outlined. In addition, a brief discussion of their applications in the fields of chemical reaction dynamics, spectroscopy, and electron scattering was presented, as well as a summary of commonly used methods by which the TDSE can be solved.

Chapter 2 developed the key theory that is applicable to general time-dependent quantum mechanics and measurement (including observables, expectation values, and flux), and introduced the concept of the wave packet as being a superposition of eigenstates. Such theory lay the foundations for discussions in later Chapters. Next, Chapter 3 built on this and delved deeper into methods used to solve the TDSE, namely the CN and SO techniques. Whilst the CN method is unconditionally stable and unitary, it was demonstrated that the SO method is far superior when applied to systems where the assumption of periodic boundary conditions is sound, owing to it being less prone to phase accumulation errors. It also has the advantage of offering a higher computational efficiency and the ability to preserve the norm of the wave packets that it propagates through time. MATLAB was used to qualify this assertion computationally by measuring the error on a Gaussian wave packet propagated using the SO method ,relative to the analytical result using the norm squared value of the difference between the wave packet values, the error on the average position, the overlap between the analytically propagated and numerically propagated wave packets, and the error in the group velocity and dispersion over time.

As detailed in Chapter 4, single eigenstates of the Hamiltonian are known as stationary states, that is, their probability densities are independent of time. Therefore, one must turn to superpositions of eigenstates (or wave packets) to access time-varying probability densities. Wave packets of PIB and QHO eigenstates were independently investigated and analysed. Chapter 5 turned the focus of the thesis to Gaussian wave packets subjected to a constant potential, which was set to zero without loss of generality. Firstly, the theory of Gaussian wave packets was developed by deriving the free particle eigenstates and eigenvalues, and the dispersion relation, in addition to how the dispersion of a wave packet depends on time, the group velocity and phase velocity. Secondly, the dispersion behaviour of Gaussian wave packets initiated with and without any net momentum was investigated. In general, dispersion over time is attributed to the distribution of momenta that comprise the overall wave packet in the superposition. Furthermore, it was also rationalised why, despite the fact that a wave packet becomes broader in the x-domain in time, its dispersion in momentum is fixed. Ultimately, this is attributed to the conservation of momentum. Finally, the interference between two travelling Gaussians was simulated to show the interference behaviour between two interacting wave packets. It was found that the wave packets reform after they have passed each other and the dispersion of each wave packet is unaffected by the interactions.

The thesis closed with a discussion of chirping with a polynomial phase as a means to control the behaviour of Gaussian wave packets in Chapter 6. Through algebraic calculations and numerical simulations, it was shown that chirping with a linear phase in k, e^{-ia_1k}, shifts the initial position of the wave packet to which it is applied by an amount proportional to a_1; the behaviour of the wave packet thereafter is analogous to that of an unchirped wave packet. However, chirping with a quadratic phase, $e^{-ia_2k^2}$, results in a shift of a wave packet in time to a non-maximally compact state with a higher degree of dispersion. If the initial position of the unchirped wave packet is centred on the origin, the the wave packet will evolve towards its maximally compact state at the origin after a time that is proportional to a_2. Beyond this time, the wave packet disperses according to the standard dispersion relation derived in Chapter 5.

Looking beyond this work, the theory of wave packets and methods of wave packet manipulation can be used to investigate the complex quantum behaviour of photoexcited molecules. Chirping provides a useful framework by which the light-matter interaction can be accurately simulated, thus enabling extensive theoretical and computational analyses into chemical phenomena. For example, the nuclear wavefunction can be localised on a desired region of a potential energy surface, such as a boundary crossing, to enhance the wavefunction amplitude at this region and more thoroughly probe non-adiabatic transitions.

Bibliography

[1] M. Simmermacher, N. E. Henriksen, K. B. Møller, A. Moreno Carrascosa and A. Kirrander, *Phys. Rev. Lett.*, 2019, **122**, 073003.

[2] E. M. Liane, M. Simmermacher and A. Kirrander, *J. Phys. B: At., Mol. Opt. Phys.*, 2024, **57**, 145602.

[3] K. Prozument, J. H. Baraban, P. B. Changala, G. B. Park, R. G. Shaver, J. S. Muenter, S. J. Klippenstein, V. Y. Chernyak and R. W. Field, *Proc. Natl. Acad. Sci. U.S.A.*, 2020, **117**, 146–151.

[4] A. R. Kurniawan, E. Suaebah and Z. A. I. Supardi, *J. Phys.: Conf. Ser.*, 2024, **2900**, 012009.

[5] M. D. Feit, J. A. Fleck and A. Steiger, *J. Comput. Phys.*, 1982, **47**, 412–433.

[6] J. Crank and P. Nicolson, *Math. Proc. Cambridge Philos. Soc.*, 1947, **43**, 50–67.

[7] A. R. Kurniawan, E. Suaebah and Z. A. I. Supardi, *J. Phys.: Conf. Ser.*, 2024, **2900**, 012009.

[8] H. D. Meyer, U. Manthe and L. S. Cederbaum, *Chem. Phys. Lett.*, 1990, **165**, 73–78.

[9] M. H. Beck, A. Jäckle, G. A. Worth and H. D. Meyer, *Phys. Rep.*, 2000, **324**, 1–105.

[10] H. Gharibnejad, B. I. Schneider, M. Leadingham and H. J. Schmale, *Comput. Phys. Commun.*, 2020, **252**, 106808.